



LUND UNIVERSITY

Application of Texture Analysis to Functional Pulmonary CT Data

Meier, Arndt; Farrow, Catherine; Harris, Benjamin; King, Gregory; Jones, Alan

Published in:
Computerized Medical Imaging and Graphics

DOI:
[10.1016/j.compmedimag.2011.01.001](https://doi.org/10.1016/j.compmedimag.2011.01.001)

2011

[Link to publication](#)

Citation for published version (APA):
Meier, A., Farrow, C., Harris, B., King, G., & Jones, A. (2011). Application of Texture Analysis to Functional Pulmonary CT Data. *Computerized Medical Imaging and Graphics*, 35(6), 438-450.
<https://doi.org/10.1016/j.compmedimag.2011.01.001>

Total number of authors:
5

General rights

Unless other specific re-use rights are stated the following general rights apply:
Copyright and moral rights for the publications made accessible in the public portal are retained by the authors and/or other copyright owners and it is a condition of accessing publications that users recognise and abide by the legal requirements associated with these rights.

- Users may download and print one copy of any publication from the public portal for the purpose of private study or research.
- You may not further distribute the material or use it for any profit-making activity or commercial gain
- You may freely distribute the URL identifying the publication in the public portal

Read more about Creative commons licenses: <https://creativecommons.org/licenses/>

Take down policy

If you believe that this document breaches copyright please contact us providing details, and we will remove access to the work immediately and investigate your claim.

LUND UNIVERSITY

PO Box 117
221 00 Lund
+46 46-222 00 00

Elsevier Editorial System(tm) for Computerized Medical Imaging and Graphics
Manuscript Draft

Manuscript Number:

Title: Application of Texture Analysis to Functional Pulmonary CT Data

Article Type: Full Length Article

Section/Category:

Keywords: texture analysis, computed tomography, asthma, COPD, lung ventilation

Corresponding Author: Dr Arndt Meier,

Corresponding Author's Institution: University of Sydney

First Author: Arndt Meier

Order of Authors: Arndt Meier; Catherine Walsh; Benjamin E Harris; Gregory G King; Allan Jones,
Dr

Manuscript Region of Origin:

Abstract: Abstract

It is demonstrated that textural parameters calculated from functional pulmonary CT data have the potential to provide a robust and objective quantitative characterisation of inhomogeneity in lung function and classification of lung diseases in routine clinical applications. Clear recommendations are made for optimum data preparation and textural parameter selection.

A new set of platform-independent software tools are presented that are implemented as plug-ins for ImageJ. The tools allow segmentation and subsequent histogram-based and grey-level co-occurrence matrix based analysis of the regions of interest. The work-flow is optimised for use in a clinical environment for the analysis of transverse Computed Tomography (CT) scans and lung

ventilation scans based on SPECT. Consistency tests are made against other texture analysis plug-ins and simulated lung CT data. The same methods are then applied to patient data consisting of a healthy reference group and one patient group each who suffered from asthma, chronic obstructive pulmonary disease (COPD), and COPD plus lung cancer. The potential for disease classification based on computer analysis is evaluated.

Application of Texture Analysis to Functional Pulmonary CT Data

Arndt Meier^a, Catherine Walsh^{b,c,d}, Benjamin E. Harris^{b,c,d}, Gregory G.King^{b,c,d}, and Allan Jones^a

a) Australian Key Centre for Microscopy and Microanalysis, The University of Sydney, Sydney 2006, NSW, Australia, email: a.meier@usyd.edu.au (*corresponding author*)

b) Department of Respiratory Medicine, Royal North Shore Hospital, St Leonards NSW 2065

c) Woolcock Inst. of Medical Research, 431 Glebe Point Road, Glebe, NSW 2037

d) Northern Clinical School, Faculty of Medicine, University of Sydney, Sydney, 2006

1 **Abstract**
2
3

4 It is demonstrated that textural parameters calculated from functional pulmonary CT data
5
6 have the potential to provide a robust and objective quantitative characterisation of
7
8 inhomogeneity in lung function and classification of lung diseases in routine clinical
9
10 applications. Clear recommendations are made for optimum data preparation and textural
11
12 parameter selection.
13
14

15
16 A new set of platform-independent software tools are presented that are implemented as plug-
17
18 ins for ImageJ. The tools allow segmentation and subsequent histogram-based and grey-level
19
20 co-occurrence matrix based analysis of the regions of interest. The work-flow is optimised
21
22 for use in a clinical environment for the analysis of transverse Computed Tomography (CT)
23
24 scans and lung ventilation scans based on SPECT. Consistency tests are made against other
25
26 texture analysis plug-ins and simulated lung CT data. The same methods are then applied to
27
28 patient data consisting of a healthy reference group and one patient group each who suffered
29
30 from asthma, chronic obstructive pulmonary disease (COPD), and COPD plus lung cancer.
31
32 The potential for disease classification based on computer analysis is evaluated.
33
34
35
36
37
38
39
40
41
42
43
44
45
46
47
48

49 **KEYWORDS:**
50

51
52 texture analysis, computed tomography, asthma, COPD, lung ventilation
53
54
55
56
57
58
59
60
61
62
63
64
65

1. Introduction

Close to 10 percent of the world population are suffering from chronic lung diseases. The two most common categories, which account for 7.7%, are asthma and chronic obstructive pulmonary disease (COPD).

According to World Health Organisation (WHO) estimates, 300 million people suffer from asthma and 255 000 people died of asthma in 2005 (WHO, 2008a) and an increase of 20% is expected over the next 10 years. Asthma is the most common chronic disease among children.

It is characterised by episodic airway narrowing that occurs on exposure to stimuli, such as exercise, dust, pollens and cold air. Asthmatic lungs are characterised by inhomogeneous ventilation when studied by pulmonary function techniques or by imaging methods. The severity of the inhomogeneity, measured by pulmonary function, is strongly related to the sensitivity of airways to inhalants, i.e. dust, pollens etc. Thus characterisation of the topographical pattern of ventilation in asthmatic lungs is important

The WHO estimates (2007), currently 210 million people suffer from chronic obstructive pulmonary disease (COPD) with 3 million people dying of COPD in 2005 (WHO, 2008b).

COPD is a chronic disease that is caused predominantly by tobacco smoking in western countries. COPD causes lung destruction, known as emphysema, and diseases of small and large airways, which result in cough, mucous production and airway narrowing with resultant breathlessness during exertion.

Single-photon emission computed tomography (SPECT) ventilation scanning (Petersson *et al.*, 2007) using Technetium-99 (TechnegasTM), is a three dimensional imaging technique used routinely in clinical nuclear medicine for diagnosis of diseases such as pulmonary embolism, when combined with imaging of blood flow (Harris *et al.*, 2007). Ventilation scans, however, have been adapted for studies of ventilation in airways disease (King *et al.*, 1997 and 1998,

1 Downie *et al.*, 2007). SPECT imaging offers the potential to characterise the topographical
2
3 distribution of ventilation so that inhomogeneity can be quantified at the regional level (Xu *et*
4
5 *al.*, 2001, Venegas *et al.*, 2005). Combining imaging information with the pulmonary function
6
7 measures of inhomogeneity will provide important information about the ventilatory
8
9 abnormalities in asthma and COPD (Tgavalekos *et al.*, 2007, Berend *et al.*, 2008). However,
10
11 suitable methods for quantifying the distribution of ventilation from SPECT data have not
12
13 been determined.
14
15
16

17
18 In this study, we investigate several potentially useful methods of quantifying the distribution
19
20 of ventilation from SPECT ventilation data using both simulated SPECT data and data from
21
22 well-described clinical groups. The new technique is based on texture analysis and can
23
24 provide an objective indicator of abnormal lung conditions.
25
26
27
28
29
30

31 **2. Methods**

32
33
34

35 We developed new techniques for multiple 3D texture analysis and conventional 3D image
36
37 analysis of clinical SPECT data of volumes representing lung tissue as identified from co-
38
39 registered CT scans that were obtained at the time of the SPECT.
40
41
42

43 The new technique uses the anatomical CT to define the lung outlines, co-registers these with
44
45 the functional SPECT data and performs an image analysis on the voxels of the SPECT thus
46
47 defined as representing lung tissue. The image analysis comprises a traditional direct analysis
48
49 of the grey levels in the SPECT slices and a texture parameters analysis derived from grey-
50
51 level co-occurrence matrices (GLCM) (Haralick, *et al.*, 1973, Choi, 2006).
52
53
54
55
56
57

58 **2.1 Simulation data**

59
60
61
62
63
64
65

1 We created a series of SPECT-V data sets based on simulated data to validate the software.

2
3 The lung phantom used in the construction of the model was based upon X-ray computed
4 tomography (CT) data from a male of height 178 cm, weighing 70 kg (Zubal *et al.*, 1994) in
5 supine position, who was chosen for his similarity to the dosimetry standard mathematical
6 phantom. The Monte Carlo simulation package used for this work was the Photon History
7 Generator (Lewellen *et al.*, 1988, Haynor *et al.*, 1991), which models the emission, scatter and
8 attenuation of photons in a heterogeneous phantom, followed by the photons' subsequent
9 collimation and detection (Chicco *et al.*, 2001).

10
11 Simulations were performed for a 23.6-mm-thick parallel-hole collimator, using a 32.5-cm
12 radius of rotation. The isotope modelled was Tc99, collected with a symmetric 20% energy
13 window centred around 140 keV into a 128×128 matrix with 120 views at equal angular
14 spacing around 360°, resulting in 5 million counts total when no defects were present. Pixel
15 resolution was 2.5mm/pixel. To test for any dependence on brightness changes we repeated
16 two simulations with 9 million counts. These settings were chosen to closely mimic typical
17 clinical settings when collecting SPECT-V data (similar contrast, spatial resolution and signal
18 to noise).

19
20 A series of studies were performed in four groups, distinguished by the size of individual
21 defects, to simulate the effects of non-ventilated lung tissue. Defects in groups 1–4 were
22 1x1x1 pixels (15 mm³), 2x2x2 pixels (125 mm³), 3x3x3 pixels (422 mm³) and 4x4x4 pixels
23 (1000 mm³) in size, respectively. These were distributed uniformly throughout both lung
24 halves in a random manner. Within each group, the amount of lung tissue involved in defects
25 varied from 0% (normal) up to 40% in steps of 5%, giving 9 studies in each group.

26
27 These simulated lung data sets were then subjected to normal clinical processing. Lungs
28 were reconstructed at the same resolution as routine SPECT data (128 slices with 128x128
29 pixels, voxel size 4.664mm³). The lung outlines were known from the original phantom and
30
31
32
33
34
35
36
37
38
39
40
41
42
43
44
45
46
47
48
49
50
51
52
53
54
55
56
57
58
59
60
61
62
63
64
65

1 converted to a binary mask which was then subjected to 2 iterations with the standard ImageJ
2
3 erosion operation using a count of 3 (minimum 3 of the nearest neighbour pixels need to be
4
5 background pixels for the present pixel to be eroded).
6
7
8
9

10 11 **2.2 Clinical data**

12
13
14 Three groups of patients were studied to evaluate the applicability of the new methods. Five
15
16 patients had asthma (data set A), and 10 current or ex-smokers that had either diagnosed
17
18 COPD (data set C) or were being evaluated for treatment of lung cancer (PELICAN¹ data set)
19
20 who had a wide range of severity of COPD, and scans from 5 patients who underwent lung
21
22 scanning for suspected pulmonary embolism but who were considered to have normal lung
23
24 scans on routine clinical assessment (data set N).
25
26
27
28

29
30 All subjects inhaled Technegas as the ventilation imaging agent. Patients had scans according
31
32 to the standard clinical protocol whereby Technegas was inhaled from the Technegas
33
34 generator by 1-2 deep inspirations followed by a breath hold to maximise Technegas particle
35
36 deposition.
37
38
39

40
41 Subjects had a ventilation SPECT scan and a CT scan acquired by a dual-detector variable
42
43 angle hybrid SPECT/CT system (Phillips SKYLight and Picker PQ5000 CT). All SPECT
44
45 studies were acquired using a 128 x 128 matrix, at 15 seconds per stop with 3 degree steps
46
47 over 360 degrees. Low-dose CT was performed using non-contrast (30mA, 10kVp, pitch 1.5,
48
49 slice thickness 4mm). Study was acquired during tidal breathing. CT images are reconstructed
50
51 using a 512 x 512 matrix with a smooth algorithm.
52
53
54

55
56 Spirometry, including the predicted forced expiratory volume during one second (FeV1), was
57
58 obtained in all groups except the normal group, using standard methods in the lung function
59

60 ¹PELICAN study: Predicting Exercise tolerance and Lung function using Imaging in patients
61 undergoing CANcer Surgery, Royal North Shore Hospital, internal study, 2007.
62
63
64
65

1 laboratory.
2
3
4
5
6

7 **2.3 Software**

8
9

10 Custom plug-ins were developed for ImageJ (Rasband, 1997-2008) to read and write CT data
11 routinely stored in Interfile data format (Craddock et al., 1989). Segmentation of the lungs in
12 the CT datasets is done with a custom written plug-in “Extract_Lungs”, which was more
13 efficient than existing segmentation plug-ins (Parker, 2008, Castleman, 2005). Segmentation
14 uses an edge-following algorithm that stays between an upper and lower grey-value threshold.
15
16
17
18
19
20
21

22 If the initial seed-point falls outside the thresholds, a new seed-point is automatically
23 determined from a search towards the median point of the previous slice and an outward spiral
24 from there if that fails.
25
26
27
28
29

30 Up to 5 regions of interest per slice are supported which are categorised as belonging to either
31 the left or right lungs. A custom-built ROI manager allows superimposition of the ROIs onto
32 SPECT ventilation data. The identified volumes are analysed for total area, mean, median,
33 modal, minimum, and maximum grey values, kurtosis, integrated optical density (IOD), and
34 histogram. Weighted means are calculated for left, right and total lung.
35
36
37
38
39
40
41

42 Anatomical CT data were registered to corresponding functional data (SPECT) with the
43 ImageJ plug-in Align3_TP (Parker, 2008) with all parameters left to their default values. The
44 outlines of the registered lung mask were then auto-detected with our segmentation algorithm
45 resulting in ImageJ standard ROIs (regions of interest). Our modified ROI manager limits all
46 subsequent analysis to within the defined ROIs.
47
48
49
50
51
52
53
54

55 From these ROIs that represent the total lung volume, GLCMs are calculated for the x, y, z,
56 and invariant orientation for a set of up to 5 chosen distances. These are then subjected to
57 standard texture analysis. We verified the correct implementation of the GLCM algorithm by
58
59
60
61
62
63
64
65

1 comparing results from an independently written plug-in [Cabrera, 2005], which calculates 4
2
3 of the 12 textural features we determine, and found both to be consistent.
4
5

6 Our methods are based on software that is easily available, widely used, modular in design,
7
8 open source and not limited to a specific operating system. ImageJ (Rasband, 1997-2008),
9
10 Abramoff *et al.*, 2004, Burger & Burge, 2008) fulfils all these criteria perfectly. And more so,
11
12 there is a very large collection of plug-ins publicly available
13
14 (<http://rsb.info.nih.gov/ij/plugins/>). The code used in this study is available from the author.
15
16
17
18
19
20
21

22 **2.4 Analysis**

23
24

25 In both the simulated and the clinical data the volumes representing lung tissue were
26
27 identified as described above. All voxels outside the eroded ROIs were excluded from the
28
29 analysis. Note that lung tissue outlines were registered to the reconstructed SPECT data, thus
30
31 avoiding any interpolation in the SPECT data set.
32
33
34

35 All SPECT data sets, simulated and clinical, were prepared in two parallel streams: *CS*
36
37 (contrast stretched) and *HM* (histogram matched). The contrast stretched data set was created
38
39 by first stretching the contrast within the 16-bit grey-levels image stack using the stack
40
41 histogram (built-in ImageJ function) and then converting the image stack to an 8-bit grey-
42
43 level image stack. The latter step used an improved version of the ImageJ Stack Converter
44
45 that uses the stack histogram as opposed to the histogram of the current slice and allows to
46
47 fold a set percentage of hot pixels into the highest remaining histogram channel. We chose the
48
49 0.02% brightest non-background pixels to be treated as hot pixels.
50
51
52
53
54

55 The histogram-matched data set used the histogram from the best ventilated simulated lung as
56
57 the reference histogram after smoothing it twice with a Gaussian filter of 5 histogram
58
59 channels width. This histogram compared well with histograms obtained from patients with
60
61
62
63
64
65

1 normal lung function. The histogram matcher we wrote uses the stack histogram and can
2
3 directly map a 16-bit image stack onto an 8-bit reference histogram thus considerably
4
5 reducing channel pile-up effects commonly encountered when first converting from 16-bit to
6
7 8-bit and then again from 8-bit to 8-bit reference histogram.
8
9

10 The 'extracted lungs' as defined by sets of ROIs were then analysed in two steps. The normal
11
12 grey value analysis calculated the total lung volume in voxels, the ventilated volume, the
13
14 minimum, mean, modal, median and maximum grey values, IOD, contrast, histogram, and
15
16 Kurtosis on a per-ROI basis. Mean values weighted by ROI area were calculated for left,
17
18 right, and total lung.
19
20
21
22
23

24 A voxel was considered to represent ventilated lung tissue if it had a grey value larger than
25
26 20% of the histogram maximum. To minimise the impact of any erratic hot pixels, the
27
28 histogram maximum was calculated from the 97% level assuming that the histogram above
29
30 97% drops with a slope of -0.5. In this work we only report the results for total lungs, but it is
31
32 noted that the software reports more details where this may be of interest.
33
34
35

36 The second step of the analysis created 8-bit grey-level co-occurrence matrices (GLCMs)
37
38 from all the ROIs of any one lung for 5 distances each: 1, 2, 4, 8, and 12 pixels (4.7, 9.3, 18.7,
39
40 37.3, 56.0mm) and for 4 direction pairs each: X (left->right, right->left), Y (top->bottom,
41
42 bottom->top), Z (up->down, down->up) and I (invariant, combining X, Y, and Z). The
43
44 invariant matrix we chose gives equal weight to each valid voxel pair and may at times differ
45
46 from a mean over the X, Y, and Z matrices as individual matrices may not have the exact
47
48 same number of voxel pairs. From these GLCMs twelve texture features were calculated as
49
50 listed in appendix A (Haralick *et al.*, 1973, Haralick 1979, Choi, 1996).
51
52
53
54
55
56
57
58
59

60 **3. Results**

61
62
63
64
65

3.1 Results from the phantom study

The texture parameters calculated from the simulated lungs show a number of correlations with the size of the defects and the total non-ventilated volume (NVV). Figure 1 illustrates this for the example of the textural parameter TC18 (coefficient of variation) and simulated defect sizes of 3x3x3 pixels. For all GLCM distances and defect sizes the parameter TC18 increases steadily with increasing NVV and more rapidly so for larger defects.

No significant differences were found between results obtained from X, Y, and Z GLCMs.

Hence only the invariant GLCMs have been studied further. For all 12 textural parameters studied we found under all conditions that the functions such as in Figure 1 are smooth and steady and that different distances in GLCM calculation result in slightly shifted versions of the same shape but that in no case does the graph of one distance cross the graph of another distance for otherwise identical settings. On the contrary, we often saw that graphs for different distances were almost undistinguishable from one another. Consequently the data from all distances were pooled into one; thus reducing the complexity of the results presented. Notwithstanding this, it is noted, that TC9 and TC30 were somewhat more sensitive to NVV changes at shorter distances and that TC2 showed no dependence on NVV but gave significantly different results for different distances.

For clarity only the relative changes in textural parameters between the lowest and highest NVV studied are reported, because the functions change smoothly with NVV and in-between values do not add much to the discussion.

Table 1 lists the relative changes in the textural parameters calculated in response to a 40% drop in ventilated lung volume. Some textural parameters are more sensitive to the changes in ventilated volume than others as can be seen from Table 1 (rows 6 and 11 “*mean*”). Also, they are typically stronger in the contrast-stretched data set (*cs*, row 6) as compared to the

1 histogram-matched data set (*hm*, row 11).
2
3

4 The results from a sensitivity test to brightness changes are shown in Table 2. We repeated the
5 simulation for the “worst” lung with a higher activity such that after adding the defects it
6 resulted in the same IOD as the perfectly ventilated simulated lung. Insensitivity to brightness
7 changes would allow the direct comparison of textural parameters derived from studies that
8 use different gamma counts. Note that rows 2 and 3 in Table 2 correspond to rows 5 and 10 in
9 Table 1 (10 mm), respectively, but the percentage changes are expressed relative to the values
10 in Table 1. It is noted that the sign of all values in Table 2 act in such a way as to reduce the
11 sensitivity of the textural parameters.
12
13
14
15
16
17
18
19
20
21
22

23 In the context of our work a good textural parameter is one that is sensitive to changes in
24 NVV or defect-size and that is at the same time insensitive to changes in brightness. With this
25 in mind we can group the textural parameters investigated into robust, intermediate and poor
26 performers:
27
28
29
30
31
32

33 **Robust textural parameters:**

34
35
36
37
38
39
40 TC13/TC31 Variance/Mean ratio: provides a solid signal of 22% change in the parameter
41 value for a 40% change in NVV while its dependence on brightness doubling is only small
42 (1.5%). The sensitivity is somewhat poorer for smaller defects.
43
44

45
46
47
48 TC30 Local homogeneity: provides still a good signal of 10.5% change for a 40% drop in
49 NVV but is more sensitive to brightness changes than the TC13/TC31 ratio (2.9%).
50

51
52
53 TC18 Coefficient of Variation: provides a very strong signal of 77% for large defects and a
54 still strong signal of 22% for small defects. It has a moderate dependence on brightness
55 changes (10.8% simulating large defects). However, correlation with clinical data discussed
56 below is excellent.
57
58
59
60
61
62
63
64
65

1
2
3
4 **Textural parameters with intermediate performance:**
5

6
7 TC1 Angular second moment: provides high sensitivity (>68%) to changes in NVV, but
8
9 unfortunately it is also very sensitive to brightness changes.
10

11
12 TC2 and TC2: Difference and inverse difference moment: show a modest sensitivity for short
13
14 distances and small-sized defects but are insensitive at larger pixel distances as well as for
15
16 larger defect sizes. However, they may be used successfully in conjunction with other
17
18 parameters to decide whether the effective size distribution of the non-ventilated volumes is
19
20 small or large.
21
22

23
24
25 TC9 Correlation: The theoretical study shows a reasonable sensitivity of around 20% to
26
27 changes twice that large in NVV but also a relatively high sensitivity to brightness changes. In
28
29 the clinical studies discussed below this parameter did not convince and is outperformed by
30
31 others.
32
33

34
35
36
37
38 **Textural parameters with poor performance:**
39

40
41 TC7, TC4, TC13, TC31, TC21, and TC23: These parameters suffer either from a lack of
42
43 sensitivity or high sensitivity to changes in brightness.
44
45

46
47
48
49 **Combination of textural parameters:**
50

51
52 The ratio of TC13/TC31 is a very good performer although neither TC13 nor TC31 are good
53
54 performers. Similarly, the ratio of TC21/TC31 gives a moderately good performance.
55
56
57

58
59
60
61 **3.2 Results from the clinical studies**
62
63
64
65

1 Figure 2 illustrates the estimated ventilated lung volume grouped by patient group. The
2
3 'normal' group shows the highest ventilated volume of about 90% and the smallest variance.
4
5 Asthmatic lungs at baseline show a slightly lower ventilated lung volume although not
6
7 statistically significant from the 'normal' lungs. The remaining patient groups show significant
8
9 reductions in ventilated lung volume that are strongest in COPD patients. There is also a
10
11 higher variability in these groups.
12
13
14
15

16 Figures 3 and 4 illustrate one of the best performing textural parameters for the 5 patient
17
18 groups studied. Both the absolute value and the variability between different GLCM distances
19
20 and between patients in the 'normal' lung function group are small (Figure 3, left panel). The
21
22 results from COPD patients which range from a mild case (right panel, c-01) to severe (c-05)
23
24 show increasingly higher values.
25
26
27
28

29 The differences between using different distances in the GLCM calculations are almost within
30
31 the numerical precision, which was also observed in the results from the simulated data. This
32
33 observation holds true for all textural parameters and patient groups studied except for TC2,
34
35 TC9 and TC30. TC9 (Correlation) and TC30 (Local Homogeneity) lose sensitivity with
36
37 increasing distance between voxel pairs and better performance is achieved by only using the
38
39 2 shortest distances (1 and 2 pixels distance corresponding to 4.7 and 9.3mm, respectively).
40
41
42
43
44
45
46
47
48
49
50
51
52
53
54
55
56
57
58
59
60
61
62
63
64
65

61
62
63
64
65

61 Pooling the data from all GLCM distances² and by patient group allows us to look for disease-
62
63 specific differences as shown in Figure 4. While asthmatics at baseline cannot be distinguished
64
65 from normal lungs, they can be clearly identified after a Metacholine challenge. PELICAN
patients and even more so COPD patients have strongly elevated values in the coefficient of
variation calculated from the GLCM.

² Except for TC9 and TC30 which pooled only the 2 shortest distances for higher sensitivity

1 Figure 5 presents the ratio of Local Homogeneity and GLCM Mean (TC30/TC31) calculated
2
3 in the same way as in the previous figure. Again, values for COPD and PELICAN patients are
4
5 significantly higher than those for normal and asthmatic lungs. It is noted, however, that
6
7 asthma patients both at baseline and at Metacholine challenge give almost identical results.
8
9 Hence combining the information from multiple textural parameters allows to distinguish
10
11 between different disease classes such as asthma from COPD.
12
13

14
15 A very strong correlation ($r^2=0.955$) between the textural parameter Coefficient of Variation
16
17 (TC18) and the estimated ventilated lung volume is illustrated in Figure 6. Similarly high
18
19 correlations of $r^2>0.8$ exist for textural parameters TC3, TC30, TC31, and the ratios
20
21 TC13/TC31 and TC21/TC31 as a function of ventilated lung volume (not illustrated). More
22
23 positive correlations ($r^2>0.49$) are observed for textural parameters TC1, TC9, and the ratio
24
25 TC1/TC31.
26
27

28
29 Independent spirometry data in the form of the predicted forced expiratory volume during 1
30
31 second (FeV1) was available for all but the 'normal' group. Again good correlations are
32
33 observed with several textural parameters ($r^2>0.5$ for TC18 and TC13/TC31, $r^2>0.4$ for TC3,
34
35 TC30, TC21/TC31, TC31 and TC1/TC31 and $r^2>0.3$ for TC1, TC2 and TC9) as illustrated in
36
37 Figure 7 for the example of TC13/TC31.
38
39

40
41 The Difference Moment (TC2) behaves differently from all other textural parameters studied.
42
43 It is insensitive to changes in both NVV and FeV1, but it is sensitive to the size distribution of
44
45 patterns in the lung. Hence the TC2 textural parameter results were prepared in a different
46
47 way. Instead of pooling the results from different GLCM distances, the parameter value
48
49 obtained with the shortest distance (1 pixel) were divided by the parameter value for the
50
51 second largest distance for any one lung and that we refer to as TC2_d for short. Data prepared
52
53 in this way resulted in a positive correlation of TC2_d with NVV ($r^2=0.69$) and a somewhat
54
55 weaker correlation with FeV1 ($r^2=0.375$).
56
57
58
59
60
61
62
63
64
65

1 All results in this section were derived from the contrast-stretched data set as it showed an
2
3 overall better performance than compared to results derived from the histogram-matched data.
4
5 It is noted that TC18, TC31 (Mean) and TC13/TC31 were indifferent to both NVV and FeV1
6
7 changes in the histogram-matched data set, but otherwise the same textural parameters
8
9 performed well as in the contrast-stretched data set. The only textural parameter that faired
10
11 significantly better in the histogram-matched data set was TC23 (Difference Entropy).
12
13
14
15
16
17
18

19 **4 Discussion**

20
21
22 Changes in the grey level distribution such as a shift to darker grey values – as can be
23
24 expected with a reduction in ventilated lung volume – is essentially removed in the histogram-
25
26 matched data. Hence, changes in the textural parameters that occur in the contrast-stretched
27
28 data set but not in the histogram-matched one are thought to be driven by histogram changes
29
30 while changes that occur in the histogram-matched data set are thought to be dominated by
31
32 changes in pattern (Table 1). Changes in the contrast-stretched data set are often a result of
33
34 both histogram and pattern changes.
35
36
37
38
39

40 In an ideal system a change in brightness should not affect the textural parameters calculated
41
42 because the GLCMs are always normalised to an IOD of unity. However, it is noted that the
43
44 spatial resolution of the observation system is significantly lower than the features that cause
45
46 them. The effective resolution in the SPECT-V data is lower than the pixel resolution of
47
48 4.664mm/pxl which in turn is much coarser than the simulated small defects starting from
49
50 2.5mm cube side length. Due to the nature of discrete sampling – and in this case significant
51
52 under-sampling – of the object space and the non-linearity of the resulting effective blurring,
53
54 the texture parameters calculated become dependent on the total optical density and contrast
55
56 in the SPECT-V data sets. This effect itself is also dependent on the effective size distribution
57
58
59
60
61
62
63
64
65

1 of the defects we seek to describe. To quantitatively describe the exact relationship is
2
3 mathematically complex and of limited practical use as it will vary from situation to situation.
4
5 Instead we seek to identify textural parameters that depend acceptably little on the variability
6
7 in patient data preparation.
8
9

10
11 The simulated data allows to fully control the environment, to know the true size distribution
12
13 of the non-ventilated lung volumes, the true ventilated volume, and to vary some of these
14
15 parameters systematically to study its impact. However, there are also some differences and
16
17 limitations compared to clinical data that are undesirable. One is that the IOD of the simulated
18
19 SPECT-V scan drops progressively with increasing NVV due to the simplicity of the model
20
21 available to us.
22
23
24
25

26
27 A patient with a smaller ventilated lung volume inhales approximately the same amount of
28
29 radioactivity as a patient with a larger ventilated lung volume. As a result the scan from the
30
31 former patient would have a larger information content³ and image contrast; because the same
32
33 amount of activity has to squeeze into a smaller volume, a wider range of different brightness
34
35 values is observed. Hence a poorly ventilated *simulated* lung has a somewhat *lower*
36
37 information content in the simulated data in contrast to a patient with a poorly ventilated lung
38
39 that would result in a *higher* information content than the ideally ventilated lung. We studied
40
41 this behaviour by simulating one data set with a higher gamma count, which resulted in an
42
43 increase of 38% in information content as opposed to a 9% drop in the non-corrected
44
45 simulation case. Although the textural parameters are modified as a result, it does not change
46
47 the overall response to NVV and we were able to identify textural parameters that are little or
48
49 non-susceptible to this change (Table 2). This finding is also directly relevant to clinical data,
50
51 because any two patients with naturally differently-sized lungs that are administered the same
52
53 amount of Technegas will have differences in contrast and information content of the SPECT
54
55
56
57
58
59

60
61 ³ We use the term information content in the strict sense of the number of grey values in an associated
62 histogram that are non-zero.
63
64
65

1 recorded. Selecting textural parameters that are insensitive to this variability in data collection
2
3 is an advantage in data interpretation.
4

5
6 Reconstructed SPECT data is routinely subjected to a rather strong smoothing filter before
7
8 being presented to a radiographer or other medical professional. Filtering at the RNSH
9
10 consists of a 9th order Butterworth filter with a cut-off of 1.2 cycles per centimetre. Since
11
12 texture analysis by definition looks at small differences in grey values between pairs of pixels,
13
14 any smoothing operation degrades the capabilities of the method for any given case. We tested
15
16 this expected behaviour by preparing both simulated and normal patient data with and
17
18 without applying the Butterworth filter and found the smoothed data set to have a poorer
19
20 sensitivity as manifested in smaller relative changes in textural parameters. We will report the
21
22 exact impact in a forthcoming separate study. In this work we only discuss reconstructed,
23
24 extracted lung data that has **not** been subjected to any post-filtering.
25
26
27
28
29
30

31 A change of distance in the calculation of the GLCMs (within reason) adds little new
32
33 information (Figure 1) with the exception of parameter TC2. In most cases the calculation of
34
35 the GLCM for only one distance seems to be sufficient. For 2 of the textural parameters
36
37 studied there is a better performance seen for shorter distances in the GLCM calculations
38
39 (TC9 and TC30). This is plausible looking at the definitions (Appendix 1). Voxel pairs that are
40
41 far from one another are unlikely to be highly correlated thus giving low correlation values in
42
43 any lung (TC9) and uniformity between them will be near the random value (TC30).
44
45
46
47

48 From the simulated data it is known that TC2_d drops with increasing defect size and in the
49
50 patient data it drops with increasing NVV. This suggests that the average size of individual,
51
52 non-ventilated areas increases with the severity of the diseases studied as opposed to a mere
53
54 increase of number of non-ventilated areas of same size. This result is consistent with the
55
56 perception of the SPECT data to the human eye.
57
58
59

60
61 Several well performing textural parameters were identified that by themselves allow to
62
63
64
65

1 distinguish between a 'normal' lung and a lung that suffers from some significant medical
2
3 condition or disease. Combinations of textural parameters have the potential to further classify
4
5 abnormal lungs. For example, to distinguish between asthmatics on one hand and COPD
6
7 patients on the other hand one can combine the results from TC18 and the ratio TC30/TC31.
8
9

10 TC18 is elevated in all diseases, but the ratio TC30/TC31 does not rise significantly in
11
12 asthmatics while it does rise significantly in COPD patients (compare Figures 4 and 5).
13
14

15
16 Correlation of several key textural parameters with the corresponding ventilated lung volume
17
18 are good to excellent for all patient data (Figures 6 and 7). Note that the ventilated lung
19
20 volume is a measure that is calculated from the original imaging data (not the GLCM), while
21
22 the FeV1 is a completely independent measurement. The pooling of data per disease group
23
24 (Figures 4 and 5) combines all patients of one disease into one - independent of the severity of
25
26 disease. Figures 6 and 7 on the other hand illustrate the relationship between reduced lung
27
28 functionality and resulting changes in derived textural parameters. It is pointed out that
29
30 reduced lung functionality goes along with higher heterogeneity in the SPECT data (Berend
31
32 *et al.*, 2008) and textural parameters that measure heterogeneity increase while parameters
33
34 that measure uniformity drop.
35
36
37
38
39

40
41 The textural parameters discussed are not all linearly independent of one another but some of
42
43 them have substantial correlations amongst them. (Clausi, 2008). For practical matters it is
44
45 desirable to identify a small number of textural parameters that give the overall best
46
47 classification performance.
48
49

50
51 TC2, TC3, TC4 and TC30 are all measures of contrast, though with different weights. TC3
52
53 and TC30, which weigh values by the inverse of the contrast (homogeneity), have both shown
54
55 consistently better performance in all patient data and either one of these two parameters are
56
57 recommend for use. As TC3 and TC30 are highly correlated one should choose only one of
58
59 them with TC3 performing marginally better in contrast-stretched data sets and TC30 better in
60
61
62
63
64
65

1 histogram-matched data sets.
2

3
4 TC1, TC21 and TC23 are all measures of orderliness. The ratio TC21/TC31 performed best in
5
6 the clinical data. The GLCM Mean (TC31) reflects brightness changes between patients that
7
8 the contrast-stretched data set is susceptible to. Thus using textural parameter combinations
9
10 that involve the GLCM Mean improves correlation in several textural parameters studied. The
11
12 histogram-matched data set shows no correlation with TC31 and combining textural
13
14 parameters with TC31 carries no advantage and TC23 by itself gives the best performance in
15
16 the group of textural parameters that measure orderliness. The value of Entropy (TC21, TC23)
17
18 increases with increasing heterogeneity.
19
20
21
22

23
24 TC9 (Correlation), TC13 (Variance), TC18 (Coefficient of Variation) and TC31 (Mean) are
25
26 descriptive statistics of the GLCMs and the frequency at which certain voxel *pairs* occur. The
27
28 combination of Variance and Mean in the Coefficient of Variation (TC18) and the Variance
29
30 over Mean ratio (TC13/TC31) gave excellent performance in the contrast-stretched data set
31
32 and is another recommended parameter for use. TC18 and the TC13/TC31 ratio are highly
33
34 correlated parameters. TC18 shows better correlation with ventilated lung volume and TC13/
35
36 TC31 shows better correlation with FeV1 but either one being a very good choice for
37
38 characterising the clinical data.
39
40
41
42

43
44 GLCM Correlation (TC9) Is largely independent of the other texture measures and has the
45
46 potential for giving additional insight. TC9 can be calculated for increasingly larger voxel
47
48 distances and the size at which the value suddenly decreases is a measure for the size of
49
50 definable objects in the original image data. However, we could not identify any 'sharp' drops
51
52 but only gradual changes with the clinical data, suggesting that there is a broad size
53
54 distribution of objects which makes this approach less powerful. Simply comparing the
55
56 differences in Correlation values between the shortest and longest distance studied with
57
58 ventilated lung volume resulted in a modest correlation ($r^2=0.41$).
59
60
61
62
63
64
65

1 It is noted that the best correlations between textural parameters and ventilated lung volume
2
3 were achieved with a linear regression while correlation with FeV1 gave consistently better
4
5 results using a logarithmic correlation function.
6
7

8
9 Summed up the following 3 recommendations can be made for the analysis of pulmonary
10
11 SPECT-V data.
12

- 13
14 1) Texture analysis sensitivity is maximised by preparing SPECT data in an unfiltered,
15
16 contrast-stretched way, as opposed to filtered or histogram-matched.
17
18
- 19
20 2) The choice of voxel pair distance in the GLCM calculation is non-critical. With
21
22 present spatial resolution in SPECT data 1, 2, or 3 pixel distances are good choices
23
24 that can also be pooled to improve statistics.
25
26
- 27
28 3) Amongst the many textural parameters studied one each should be chosen from 3
29
30 different groups of parameters to balance the capability to characterise with the
31
32 computational effort involved. These are the textural parameters TC18 or the ratio
33
34 TC13/TC31 from the descriptive statistics group, the parameter TC3 or TC30 from the
35
36 TC13/TC31 from the descriptive statistics group, the parameter TC3 or TC30 from the
37
38 contrast group and the parameter ratio TC21/TC31 in the orderliness group.
39

40 Application of the new software package is not limited to pulmonary studies – in fact it may
41
42 also be applied to other organs or to completely different fields such as material sciences or
43
44 mineralogy. However, in its present form the software package is optimized to the work-flow
45
46 of studying lungs in a clinical scenario.
47
48

49 50 51 52 53 **Summary**

54
55 It has been demonstrated that a textural parameter analysis of functional pulmonary CT data
56
57
58
59 has the potential to provide a robust and objective quantitative characterisation of
60
61
62
63
64
65

1 inhomogeneity in lung function and classification of lung diseases with application in routine
2
3 clinical applications and national screening programmes. The new methods applied to SPECT
4
5 lung ventilation scans are capable of distinguishing between different types of diseases.
6
7 Strong correlations between key textural parameters and independent lung function data such
8
9 as the FeV1 suggest that a quantitative description of the severity of diseases such as asthma
10
11 or COPD by means of derived texture parameters is viable. Clear recommendations have been
12
13 made for optimum data preparation and textural parameter selection. In a forthcoming study
14
15 we plan to use data from larger numbers of patients and additional spirometry data to further
16
17 refine the methods.
18
19
20
21
22
23
24
25

26 **Acknowledgements**

27
28
29 This work is supported by the Australian Research Council through the ARC Linkage Project
30
31 LP0562715. The authors are grateful for scientific and technical input and support from the
32
33 Australian Microscopy & Microanalysis Research Facility (AMMRF) node at
34
35 the University of Sydney. We also like to thank the staff at the Royal North Shore Hospital
36
37 that helped in the data collection and the volunteer patients that participated in this study. In
38
39 particular we like to thank Peter Chicco, Department of Biomedical Engineering, who
40
41 provided the lung simulations, Dale and Elizabeth Bailey, Department of Nuclear Medicine,
42
43 for discussion and data conversion.
44
45
46
47
48

49
50 We like to thank Wayne Rasband and all other developers that made contributions to ImageJ
51
52 and its plug-ins for sharing their work freely with other researchers (Rasband, 1997-2008,
53
54 Abramoff *et al.*, 2004) – without them our work would have been much harder. Part of the
55
56 software presented here started their development based on other publicly available plug-ins
57
58 that are accessible through the ImageJ web page (Rasband,1997-2008, Castleman, 2005,
59
60
61
62
63
64
65

1 Miller, 2002).
 2
 3
 4
 5

6 **References**

- 7 Abramoff, MD, Magelhaes, PJ, Ram, SJ, Image Processing with ImageJ, Biophotonics
 8 International (2004), **11**(7):36-42
 9
 10 Berend N, Salome CM, King GG, Mechanisms of airway hyper-responsiveness in asthma.
 11 Respirology (2008), **13**(5):624-631
 12
 13 Burger W and Burge MJ, Digital Image Processing - An Algorithmic Approach using Java.
 14 Springer-Verlag, New York (2008). ISBN 978-1-84628-379-6, www.imagingbook.com
 15
 16 Cabrera JE, “GLCM_Texture” plug-in for ImageJ, (2005), <http://rsb.info.nih.gov/ij/plugins/>
 17
 18 Castleman M, “Cell_outliner” plug-in for ImageJ (m@mlcastle.net), Columbia University
 19 (2005) <http://rsb.info.nih.gov/ij/plugins/cell-outliner.html>
 20
 21 Chicco P, Magnussen JS, Mackey DW, Bush V, Emmett L, Storey G, Bautovich G, and Wall
 22 H van der, SPET of a computerised model of diffuse lung disease, Eur.J.Nuc.Med (2001),
 23 **28**(2):150-154
 24
 25 Choi HK, New Methods for Image Analysis of Tissue Sections. PhD thesis, Uppsala
 26 University, Sweden (1996), ISBN 91-554-3829-6
 27
 28 Clausi DA, An analysis of co-occurrence texture statistics as a function of grey level
 29 quantization. Can. J. Remote Sensing, (2002), **28**(1):45–62
 30
 31 Craddock TD, Bailey DL, Hutton BF, Conninck F De, Busemann-Sokole E, Bergmann H, and
 32 Noelpp U, A standard protocol for the exchange of nuclear medicine image files.
 33 NucMedComm (1989), **10**:703-713
 34
 35 Downie SR, Salome CM, Verbanck S, Thompson BR, Berend N and King GG, Ventilation
 36 heterogeneity is a major determinant of airway hyperresponsiveness in asthma, independent
 37 of airway inflammation. Thorax (2007), **62**:684-689
 38
 39 Haralick RM, Shanmugam K, and Dinstein I, Textural features for image classification. IEEE
 40 Transactions on Systems, Man, and Cybernetics (1973), SMC-**3**(6):610-621
 41
 42 Haralick RM, Statistical and structural approaches to texture. Proceedings of the IEEE 67
 43 (1979), **5**:786-804
 44
 45 Harris BE, Bailey D, Miles S, Bailey E, Rogers K, Roach P, Thomas P, Hensley M, and King
 46 GG, “Objective analysis of tomographic ventilation perfusion scintigraphy in pulmonary
 47 embolism”, Am. J. Respir. Crit. Care Med. , March 15, 2007
 48
 49 Haynor DR, Harrison RL, Lewellen TK, The use of importance sampling techniques to
 50 improve the efficiency of photon tracking in emission tomography simulations. Med Phys
 51 (1991), **18**:990–1001
 52
 53 King GG, Eberl S, Salome CM, Meikle SR, and Woolcock AJ, Airway closure measured by a
 54 Technegas bolus and SPECT. Am.J.Respir.Crit.CareMed. (1997) **155**:682–688
 55
 56 King GG, Eberl S, Salome CM, Young IH, and Woolcock AJ, Differences in airway closure
 57 between normal and asthmatic subjects measured with single-photon emission computed
 58 tomography and technegas. Am.J.Respir.Crit.CareMed. (1998), **158**:1900–1906.
 59
 60 Lewellen TK, Anson CP, Haynor DR, Design of a simulation system for emission
 61
 62
 63
 64
 65

1 tomographs. *J Nucl Med* (1988), **29**:871
 2
 3 Miller M, “Segmenting_Assistant”, plug-in for ImageJ, (2002) mmiller3@iupui.edu,
 4 <http://rsb.info.nih.gov/ij/plugins/index.html>
 5
 6 Parker JA, Align3_TP: stack alignment plug-in for ImageJ, J.A.Parker@IEEE.org (version
 7 25/Mar/2008), <http://www.med.harvard.edu/JPNM/ij/plugins/Align3TP.html>
 8
 9 Petersson J, Sánchez-Crespo A, Larsson SA and Mure M, Physiological imaging of the lung:
 10 single-photon-emission computed tomography (SPECT). *J Appl Physiol* (2007) **102**:468-476
 11
 12 Rasband, W.S., ImageJ, U. S. National Institutes of Health, Bethesda, Maryland, USA,
 13 <http://rsb.info.nih.gov/ij/>, 1997-2008.
 14
 15 Tgavalekos NT, Musch G, Harris RS, Vidal Melo MF, Winkler T, Schroeder T, Callahan R,
 16 Lutchen KR and Venegas JG, Relationship between airway narrowing, patchy ventilation and
 17 lung mechanics. *Eur Respir J* (2007), **29**:1174–1181
 18
 19 Venegas JG, Schroeder T, Harris S, Winkler RT, and Vidal Melo MF, The distribution of
 20 ventilation during bronchoconstriction is patchy and bimodal: A PET imaging study.
 21 *Respiratory Physiology & Neurobiology* (2005) **148**:57–64
 22
 23 WHO World Health Organisation, 2008a, <http://www.who.int/respiratory/asthma/en/>
 24
 25 WHO World Health Organisation, 2008b, <http://www.who.int/respiratory/copd/en/>
 26
 27 Xu J, Moonen M, Johansson Å, Gustafsson A, and Bake B, Quantitative analysis of
 28 inhomogeneity in ventilation SPET. *Eur J Nucl Med* (2001) **28**:1795–1800
 29
 30 Zubal IG, Harrell CR, Smith EO, Rattner Z, Gindi G, Hoffer PB, Computerized three-
 31 dimensional segmented human anatomy. *Med Phys* (1994), **21**:299–302
 32
 33
 34
 35
 36
 37
 38
 39
 40
 41
 42
 43
 44
 45
 46
 47
 48
 49
 50
 51
 52
 53
 54
 55
 56
 57
 58
 59
 60
 61
 62
 63
 64
 65

Appendix A: Definition of textural features from the co-occurrence matrix

A co-occurrence matrix $P(i,j|d,\theta)$ (PM for short) contains the probability that the grey level i occurs at a distance d in direction θ from a pixel with grey value j . N is the size of the co-occurrence matrix ($N=256$ in this study). Integrated sums are calculated from the matrix variance. We further define the vertical ($p_x(i)$), horizontal ($p_y(i)$), minor diagonal ($p_{x-y}(k)$) sums, the vertical (μ_x) and horizontal (μ_y) mean, and the variance of the vertical (V_x) and horizontal (V_y) directions (Choi, 1996). Note that the GLCM mean is distinct from the mean grey value of the original image because it is weighted by the frequency of occurrence *in combination with* a certain neighbour pixel value.

$$P_x(i) = \sum_{j=0}^{N-1} PM, \quad P_y(i) = \sum_{i=0}^{N-1} PM, \quad P_{x-y}(k) = \sum_{i=0, |i-j|=k}^{N-1} \sum_{j=0}^{N-1} PM, \quad \mu_x = \sum_i i P_x(i),$$

$$\mu_y = \sum_j j P_y(j), \quad V_x = \sum_i (i - \mu_x)^2 P_x(i), \quad V_y = \sum_j (j - \mu_y)^2 P_y(j)$$

TC_1 Angular Second Moment $\sum_{i=0}^{N-1} \sum_{j=0}^{N-1} PM^2$

TC_2 Difference Moment or GLCM Contrast $\sum_{i=0}^{N-1} \sum_{j=0}^{N-1} (i-j)^2 PM$

TC_3 Inverse Difference Moment, $\sum_{i=0}^{N-1} \sum_{j=0}^{N-1} (1+(i-j)^2)^{-1} PM$

TC_4 Diagonal Moment, $\sum_{i=0}^{N-1} \sum_{j=0}^{N-1} \sqrt{0.5(i-j)} PM$

TC_7 Inertia, $\sum_{n=0}^{N-1} n^2 \left(\sum_{i=0, |i-j|=n}^{N-1} \sum_{j=0}^{N-1} (i-j)^2 PM \right)$

TC_9 GLCM Correlation, $\left(\sum_{i=0}^{N-1} \sum_{j=0}^{N-1} (ij) PM - \mu_x \mu_y \right) / \sqrt{V_x V_y}$

TC13 GLCM Variance, V_x

TC18 Coefficient of Variation, $\sqrt{V_x V_y} / \mu_x \mu_y$

TC21 Entropy, $\sum_{i=0}^{N-1} \sum_{j=0}^{N-1} (PM) (-\ln(PM))$

TC23 Difference Entropy, $\sum_{i=0}^{N-1} P_{x-y}(i) \log_e(P_{x-y}(i))$

TC30 Local Homogeneity, $\sum_{n=0}^{N-1} (P_{x-y}(n) / (1+n^2))$

TC31 GLCM Mean $0.5 \cdot (\mu_x + \mu_y)$

histogram	cube side length in [mm]	TC_1 Angular Second Moment	TC_3 Inverse Different Moment	TC_4 Diagonal Moment	TC_9 Correlation	TC18 Coefficient of Variation	TC21 Entropy	TC30 Local Homogeneity	TC13 Sum of squares / Variance	TC31 Mean	TC13/TC31 Variance /Mean ratio
cs	2.5	111.9	4.2	-27.1	-15.2	22.5	-8.4	4.2	-2.2	-10.6	9.5
cs	5.0	106.4	7.5	-27.3	-20.0	28.9	-8.0	7.5	-16.8	-19.6	3.5
cs	7.5	85.8	9.0	-23.3	-22.3	46.6	-6.7	9.0	-17.7	-25.1	9.8
cs	10.0	68.6	10.5	-20.2	-19.2	77.0	-5.6	10.5	-15.6	-30.9	22.2
cs	mean	93.2	7.8	-24.5	-19.2	43.7	-7.2	7.8	-13.1	-21.6	11.3
hm	2.5	111.9	2.3	-27.2	-11.7	-0.7	-8.4	2.3	-0.4	0.1	-0.6
hm	5.0	106.4	-0.4	-24.9	-15.6	-0.1	-8.0	-0.4	-0.3	-0.1	-0.2
hm	7.5	85.8	0.4	-21.5	-16.1	-1.0	-6.8	0.4	-1.3	-0.2	-1.1
hm	10.0	68.6	2.1	-18.7	-13.8	0.1	-5.6	2.1	-1.1	-0.6	-0.5
hm	mean	93.2	1.1	-23.1	-14.3	-0.4	-7.2	1.1	-0.8	-0.2	-0.6

Table 1: Sensitivity of textural parameters to a 40% reduction in ventilated lung volume. The latter was achieved by randomly inserting black cubes of side length 2.5, 5, 7.5 and 10mm into the simulated lung. Results are shown as relative changes in the textural parameter for either preparing the data in a histogram-matched (hm) or a contrast-stretched (cs) way and as a mean over 5 distances used in the GLCM calculation.

Histogram	TC 1 Angular Second Moment	TC 3 Inverse Different Moment	TC 4 Diagonal Moment	TC 9 Corre lation	TC18 Coefficient of Variation	TC21 Entro py	TC30 Local Homog eneity	TC13 Sum of squares (Variance)	TC31 Mean	TC13/ TC31 Variance /Mean ratio
cs	-62.6	-2.9	53.4	10.8	-10.8	11.5	-2.9	8.7	10.4	-1.5
hm	-62.3	-3.9	48.5	9.0	0.5	11.3	-3.9	-0.1	-0.3	0.2

Table 2: Sensitivity of textural parameters to a 40% increase in gamma counts. The simulated defects have a cube side length of 10mm. Listed are the differences in the values of the textural parameters derived from either the standard simulation with 40% NVV and associated drop in average brightness and an alternative simulation with a higher gamma count such that after knocking out 40% of the ventilated volume the IOD matched the IOD of the perfectly ventilated lung simulation.

Figure captions

Figure 1: Illustration of textural parameter TC18, Coefficient of Variation, from the simulation study for cube-shaped defects of size 7.5mm cube side length as a function of non-ventilated lung volume in percent. The GLCMs were created for 5 pixel distances each (1, 2, 4, 8, 12 pixels) corresponding to distances in the lung of 4.7, 9.3, 18.7, 37.3 and 56.0mm, respectively. The coefficient of variation is larger for small pixel distances and increases with NVV and more rapidly so for larger defects (not illustrated).

Figure 2: Relative ventilated lung volume (solid black) and standard variation (hashed) per patient group.

Figure 3: Illustration of textural parameter TC18, the Coefficient of Variation, for a set of 5 'normal' lungs (left) and a set of 5 lungs of patients suffering from COPD (right). The severity of COPD increases from top to bottom.

Figure 4: Textural parameter 18 (solid black) and standard deviation (hashed) from the invariant GLCM and for all 5 distances for the 5 patient groups studied

Figure 5: Ratio of textural parameter 30/31 (solid black) and standard deviation (hashed) from the invariant GLCM and mean over 5 distances for the 5 patient groups studied

Figure 6: High correlation between ventilated lung volume in percent and textural parameter 18 (coefficient of variation) ($r^2=0.955$).

Figure 7: Correlation between textural parameter TC13/TC31 (Variance over Mean ratio) and independent spirometry data (FeV1) for 4 of the 5 patient groups. No spirometry data was available for the 'normal' group. The quality of the linear regression is $r^2=0.66$.

FIGURE 1

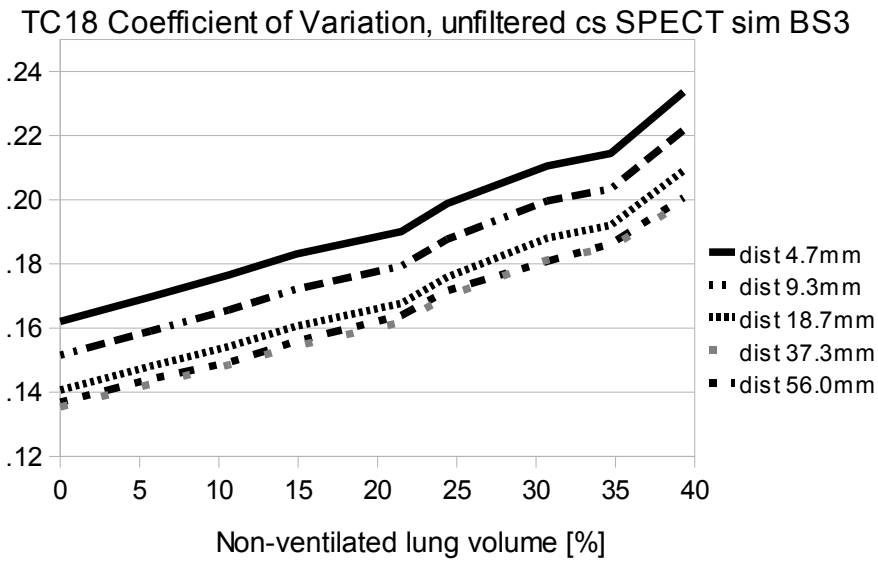


FIGURE 2

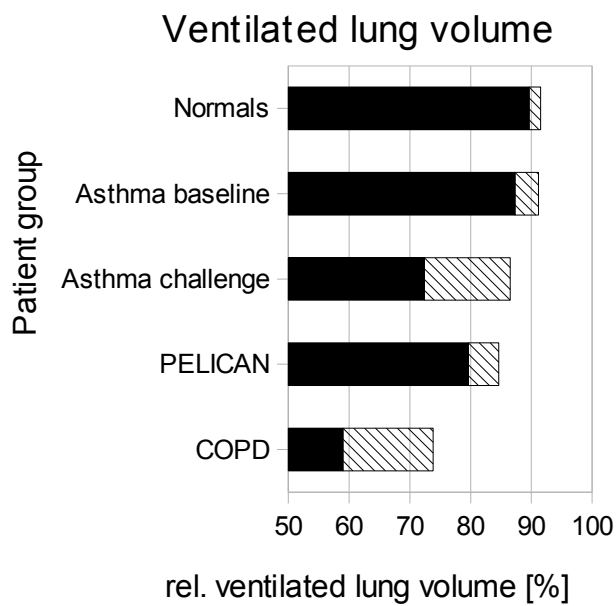


FIGURE 3 (left and right panel, reproduction in black-and-white)

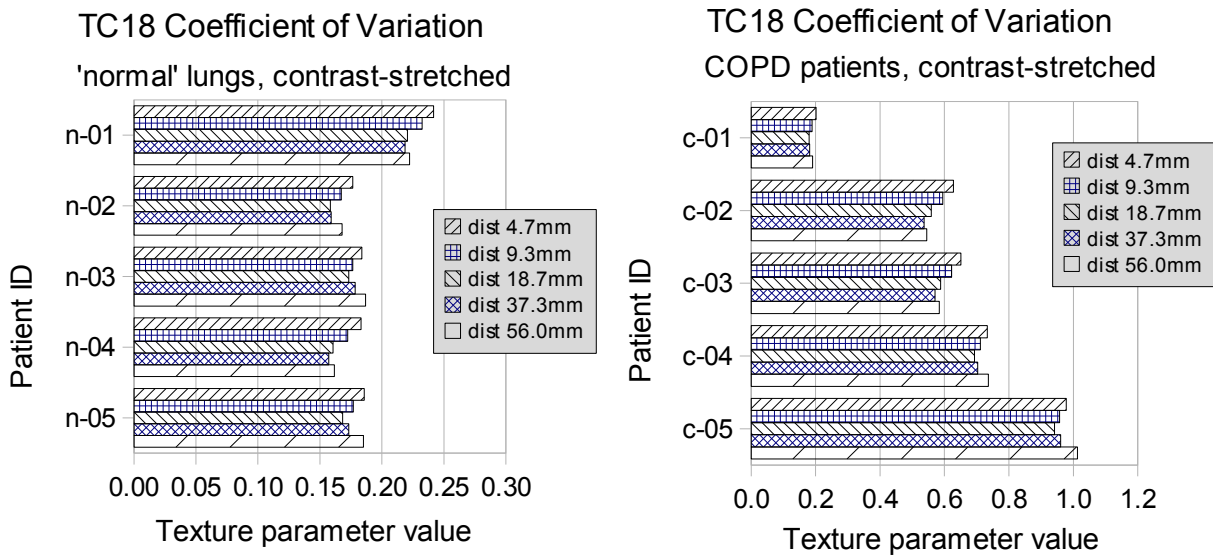


FIGURE 4

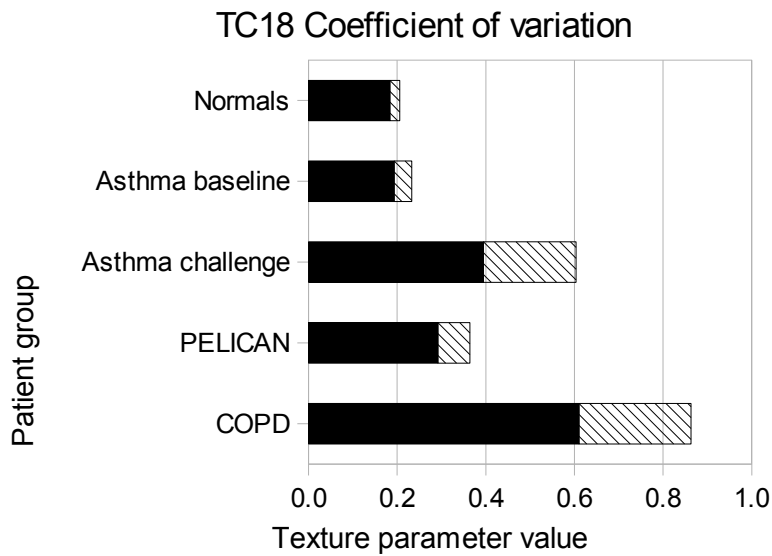


FIGURE 5

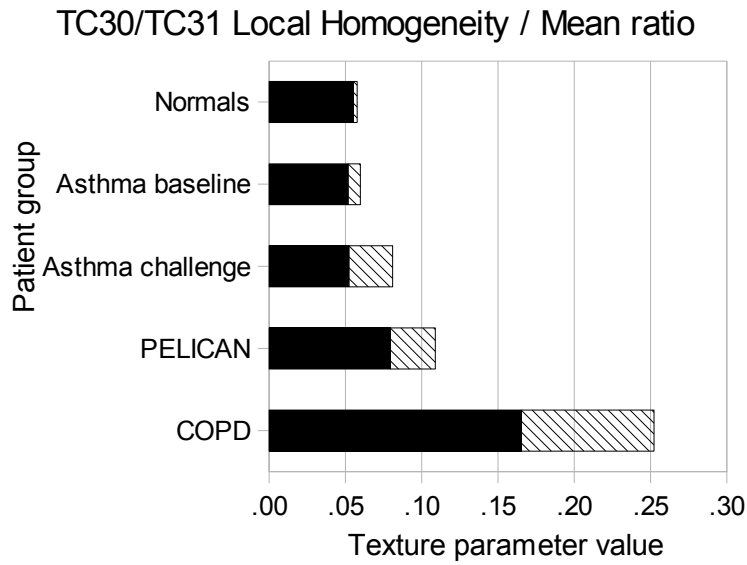


FIGURE 6 (colour reproduction for web-publishing, black-and-white for print)

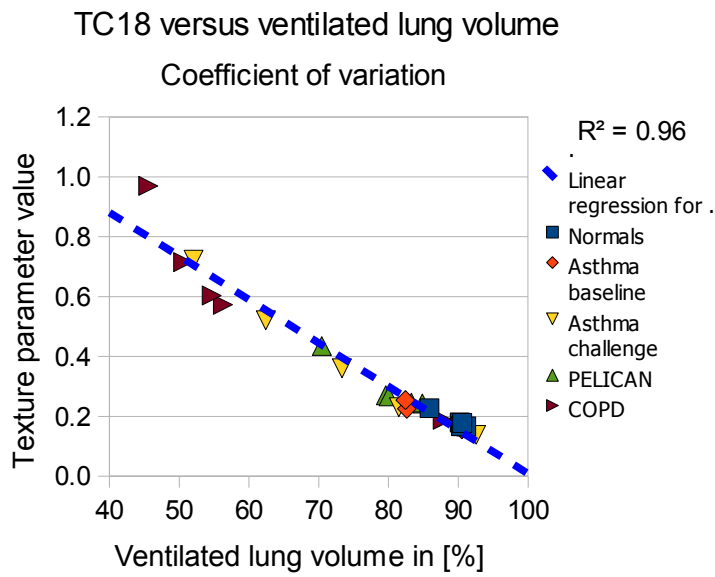
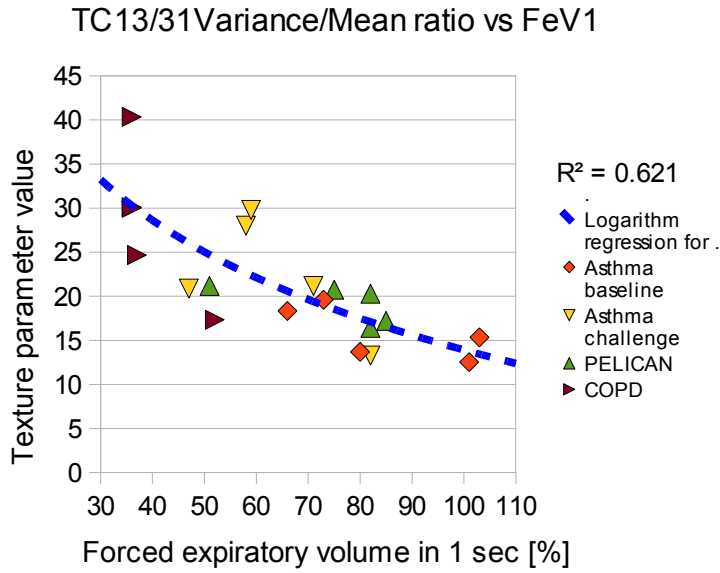


FIGURE 7 (colour reproduction for web-publishing, black-and-white for print)



Application of Texture Analysis to Functional Pulmonary CT Data

Arndt Meier^a, Catherine Walsh^{b,c,d}, Benjamin E. Harris^{b,c,d}, Gregory G.King^{b,c,d}, and Allan Jones^a

a) Australian Key Centre for Microscopy and Microanalysis, The University of Sydney, Sydney 2006, NSW, Australia, email: a.meier@usyd.edu.au (*corresponding author*)

b) Department of Respiratory Medicine, Royal North Shore Hospital, St Leonards NSW 2065

c) Woolcock Inst. of Medical Research, 431 Glebe Point Road, Glebe, NSW 2037

d) Northern Clinical School, Faculty of Medicine, University of Sydney, Sydney, 2006

1 **Abstract**
2
3

4 It is demonstrated that textural parameters calculated from functional pulmonary CT data
5 have the potential to provide a robust and objective quantitative characterisation of
6 inhomogeneity in lung function and classification of lung diseases in routine clinical
7 applications. Clear recommendations are made for optimum data preparation and textural
8 parameter selection.
9

10
11
12 A new set of platform-independent software tools are presented that are implemented as plug-
13 ins for ImageJ. The tools allow segmentation and subsequent histogram-based and grey-level
14 co-occurrence matrix based analysis of the regions of interest. The work-flow is optimised
15 for use in a clinical environment for the analysis of transverse Computed Tomography (CT)
16 scans and lung ventilation scans based on SPECT. Consistency tests are made against other
17 texture analysis plug-ins and simulated lung CT data. The same methods are then applied to
18 patient data consisting of a healthy reference group and one patient group each who suffered
19 from asthma, chronic obstructive pulmonary disease (COPD), and COPD plus lung cancer.
20
21
22 The potential for disease classification based on computer analysis is evaluated.
23
24
25
26
27
28
29
30
31
32
33
34
35
36
37
38
39
40
41
42
43
44
45
46
47
48

49 **KEYWORDS:**
50

51
52 texture analysis, computed tomography, asthma, COPD, lung ventilation
53
54
55
56
57
58
59
60
61
62
63
64
65

1. Introduction

Close to 10 percent of the world population are suffering from chronic lung diseases. The two most common categories, which account for 7.7%, are asthma and chronic obstructive pulmonary disease (COPD).

According to World Health Organisation (WHO) estimates, 300 million people suffer from asthma and 255 000 people died of asthma in 2005 (WHO, 2008a) and an increase of 20% is expected over the next 10 years. Asthma is the most common chronic disease among children.

It is characterised by episodic airway narrowing that occurs on exposure to stimuli, such as exercise, dust, pollens and cold air. Asthmatic lungs are characterised by inhomogeneous ventilation when studied by pulmonary function techniques or by imaging methods. The severity of the inhomogeneity, measured by pulmonary function, is strongly related to the sensitivity of airways to inhalants, i.e. dust, pollens etc. Thus characterisation of the topographical pattern of ventilation in asthmatic lungs is important

The WHO estimates (2007), currently 210 million people suffer from chronic obstructive pulmonary disease (COPD) with 3 million people dying of COPD in 2005 (WHO, 2008b).

COPD is a chronic disease that is caused predominantly by tobacco smoking in western countries. COPD causes lung destruction, known as emphysema, and diseases of small and large airways, which result in cough, mucous production and airway narrowing with resultant breathlessness during exertion.

Single-photon emission computed tomography (SPECT) ventilation scanning (Petersson *et al.*, 2007) using Technetium-99 (TechnegasTM), is a three dimensional imaging technique used routinely in clinical nuclear medicine for diagnosis of diseases such as pulmonary embolism, when combined with imaging of blood flow (Harris *et al.*, 2007). Ventilation scans, however, have been adapted for studies of ventilation in airways disease (King *et al.*, 1997 and 1998,

1 Downie *et al.*, 2007). SPECT imaging offers the potential to characterise the topographical
2
3 distribution of ventilation so that inhomogeneity can be quantified at the regional level (Xu *et*
4
5 *al.*, 2001, Venegas *et al.*, 2005). Combining imaging information with the pulmonary function
6
7 measures of inhomogeneity will provide important information about the ventilatory
8
9 abnormalities in asthma and COPD (Tgavalekos *et al.*, 2007, Berend *et al.*, 2008). However,
10
11 suitable methods for quantifying the distribution of ventilation from SPECT data have not
12
13 been determined.
14
15
16
17

18 In this study, we investigate several potentially useful methods of quantifying the distribution
19
20 of ventilation from SPECT ventilation data using both simulated SPECT data and data from
21
22 well-described clinical groups. The new technique is based on texture analysis and can
23
24 provide an objective indicator of abnormal lung conditions.
25
26
27
28
29
30
31

32 **2. Methods**

33
34

35 We developed new techniques for multiple 3D texture analysis and conventional 3D image
36
37 analysis of clinical SPECT data of volumes representing lung tissue as identified from co-
38
39 registered CT scans that were obtained at the time of the SPECT.
40
41
42

43 The new technique uses the anatomical CT to define the lung outlines, co-registers these with
44
45 the functional SPECT data and performs an image analysis on the voxels of the SPECT thus
46
47 defined as representing lung tissue. The image analysis comprises a traditional direct analysis
48
49 of the grey levels in the SPECT slices and a texture parameters analysis derived from grey-
50
51 level co-occurrence matrices (GLCM) (Haralick, *et al.*, 1973, Choi, 2006).
52
53
54
55
56
57
58

59 **2.1 Simulation data**

60
61
62
63
64
65

1 We created a series of SPECT-V data sets based on simulated data to validate the software.

2
3 The lung phantom used in the construction of the model was based upon X-ray computed
4 tomography (CT) data from a male of height 178 cm, weighing 70 kg (Zubal *et al.*, 1994) in
5 supine position, who was chosen for his similarity to the dosimetry standard mathematical
6 phantom. The Monte Carlo simulation package used for this work was the Photon History
7 Generator (Lewellen *et al.*, 1988, Haynor *et al.*, 1991), which models the emission, scatter and
8 attenuation of photons in a heterogeneous phantom, followed by the photons' subsequent
9 collimation and detection (Chicco *et al.*, 2001).

10
11 Simulations were performed for a 23.6-mm-thick parallel-hole collimator, using a 32.5-cm
12 radius of rotation. The isotope modelled was Tc99, collected with a symmetric 20% energy
13 window centred around 140 keV into a 128×128 matrix with 120 views at equal angular
14 spacing around 360°, resulting in 5 million counts total when no defects were present. Pixel
15 resolution was 2.5mm/pixel. To test for any dependence on brightness changes we repeated
16 two simulations with 9 million counts. These settings were chosen to closely mimic typical
17 clinical settings when collecting SPECT-V data (similar contrast, spatial resolution and signal
18 to noise).

19
20 A series of studies were performed in four groups, distinguished by the size of individual
21 defects, to simulate the effects of non-ventilated lung tissue. Defects in groups 1–4 were
22 1x1x1 pixels (15 mm³), 2x2x2 pixels (125 mm³), 3x3x3 pixels (422 mm³) and 4x4x4 pixels
23 (1000 mm³) in size, respectively. These were distributed uniformly throughout both lung
24 halves in a random manner. Within each group, the amount of lung tissue involved in defects
25 varied from 0% (normal) up to 40% in steps of 5%, giving 9 studies in each group.

26
27 These simulated lung data sets were then subjected to normal clinical processing. Lungs
28 were reconstructed at the same resolution as routine SPECT data (128 slices with 128x128
29 pixels, voxel size 4.664mm³). The lung outlines were known from the original phantom and
30
31
32
33
34
35
36
37
38
39
40
41
42
43
44
45
46
47
48
49
50
51
52
53
54
55
56
57
58
59
60
61
62
63
64
65

1 converted to a binary mask which was then subjected to 2 iterations with the standard ImageJ
2
3 erosion operation using a count of 3 (minimum 3 of the nearest neighbour pixels need to be
4
5 background pixels for the present pixel to be eroded).
6
7
8
9

10 11 **2.2 Clinical data**

12
13
14 Three groups of patients were studied to evaluate the applicability of the new methods. Five
15
16 patients had asthma (data set A), and 10 current or ex-smokers that had either diagnosed
17
18 COPD (data set C) or were being evaluated for treatment of lung cancer (PELICAN¹ data set)
19
20 who had a wide range of severity of COPD, and scans from 5 patients who underwent lung
21
22 scanning for suspected pulmonary embolism but who were considered to have normal lung
23
24 scans on routine clinical assessment (data set N).
25
26
27
28

29
30 All subjects inhaled Technegas as the ventilation imaging agent. Patients had scans according
31
32 to the standard clinical protocol whereby Technegas was inhaled from the Technegas
33
34 generator by 1-2 deep inspirations followed by a breath hold to maximise Technegas particle
35
36 deposition.
37
38
39

40
41 Subjects had a ventilation SPECT scan and a CT scan acquired by a dual-detector variable
42
43 angle hybrid SPECT/CT system (Phillips SKYLIGHT and Picker PQ5000 CT). All SPECT
44
45 studies were acquired using a 128 x 128 matrix, at 15 seconds per stop with 3 degree steps
46
47 over 360 degrees. Low-dose CT was performed using non-contrast (30mA, 10kVp, pitch 1.5,
48
49 slice thickness 4mm). Study was acquired during tidal breathing. CT images are reconstructed
50
51 using a 512 x 512 matrix with a smooth algorithm.
52
53
54

55
56 Spirometry, including the predicted forced expiratory volume during one second (FeV1), was
57
58

59
60 ¹ PELICAN study: Predicting Exercise tolerance and Lung function using Imaging in
61 patients undergoing CANCER Surgery, Royal North Shore Hospital, internal study, 2007.
62
63
64
65

1 obtained in all groups except the normal group, using standard methods in the lung function
2
3 laboratory.
4
5
6
7
8

9 **2.3 Software**

10 Custom plug-ins were developed for ImageJ (Rasband, 1997-2008) to read and write CT data
11
12 routinely stored in Interfile data format (Craddock et al., 1989). Segmentation of the lungs in
13
14 the CT datasets is done with a custom written plug-in “Extract_Lungs”, which was more
15
16 efficient than existing segmentation plug-ins (Parker, 2008, Castleman, 2005). Segmentation
17
18 uses an edge-following algorithm that stays between an upper and lower grey-value threshold.
19
20 If the initial seed-point falls outside the thresholds, a new seed-point is automatically
21
22 determined from a search towards the median point of the previous slice and an outward
23
24 spiral from there if that fails.
25
26
27
28
29
30

31
32 Up to 5 regions of interest per slice are supported which are categorised as belonging to either
33
34 the left or right lungs. A custom-built ROI manager allows superimposition of the ROIs onto
35
36 SPECT ventilation data. The identified volumes are analysed for total area, mean, median,
37
38 modal, minimum, and maximum grey values, kurtosis, integrated optical density (IOD), and
39
40 histogram. Weighted means are calculated for left, right and total lung.
41
42
43
44

45 Anatomical CT data were registered to corresponding functional data (SPECT) with the
46
47 ImageJ plug-in Align3_TP (Parker, 2008) with all parameters left to their default values. The
48
49 outlines of the registered lung mask were then auto-detected with our segmentation algorithm
50
51 resulting in ImageJ standard ROIs (regions of interest). Our modified ROI manager limits all
52
53 subsequent analysis to within the defined ROIs.
54
55
56
57

58 From these ROIs that represent the total lung volume, GLCMs are calculated for the x, y, z,
59
60 and invariant orientation for a set of up to 5 chosen distances. These are then subjected to
61
62
63
64
65

1 standard texture analysis. We verified the correct implementation of the GLCM algorithm by
2
3 comparing results from an independently written plug-in [Cabrera, 2005], which calculates 4
4
5 of the 12 textural features we determine, and found both to be consistent.
6
7

8
9 Our methods are based on software that is easily available, widely used, modular in design,
10
11 open source and not limited to a specific operating system. ImageJ (Rasband, 1997-2008),
12
13 Abramoff *et al.*, 2004, Burger & Burge, 2008) fulfils all these criteria perfectly. And more so,
14
15 there is a very large collection of plug-ins publicly available
16
17 (<http://rsb.info.nih.gov/ij/plugins/>). The code used in this study is available from the author.
18
19
20
21
22
23

24 **2.4 Analysis**

25
26
27 In both the simulated and the clinical data the volumes representing lung tissue were
28
29 identified as described above. All voxels outside the eroded ROIs were excluded from the
30
31 analysis. Note that lung tissue outlines were registered to the reconstructed SPECT data, thus
32
33 avoiding any interpolation in the SPECT data set.
34
35
36

37
38 All SPECT data sets, simulated and clinical, were prepared in two parallel streams: *CS*
39
40 (contrast stretched) and *HM* (histogram matched). The contrast stretched data set was created
41
42 by first stretching the contrast within the 16-bit grey-levels image stack using the stack
43
44 histogram (built-in ImageJ function) and then converting the image stack to an 8-bit grey-
45
46 level image stack. The latter step used an improved version of the ImageJ Stack Converter
47
48 that uses the stack histogram as opposed to the histogram of the current slice and allows to
49
50 fold a set percentage of hot pixels into the highest remaining histogram channel. We chose the
51
52 0.02% brightest non-background pixels to be treated as hot pixels.
53
54
55
56

57
58 The histogram-matched data set used the histogram from the best ventilated simulated lung as
59
60 the reference histogram after smoothing it twice with a Gaussian filter of 5 histogram
61
62
63
64
65

1 channels width. This histogram compared well with histograms obtained from patients with
2
3 normal lung function. The histogram matcher we wrote uses the stack histogram and can
4
5 directly map a 16-bit image stack onto an 8-bit reference histogram thus considerably
6
7 reducing channel pile-up effects commonly encountered when first converting from 16-bit to
8
9 8-bit and then again from 8-bit to 8-bit reference histogram.

10
11
12
13 The 'extracted lungs' as defined by sets of ROIs were then analysed in two steps. The normal
14
15 grey value analysis calculated the total lung volume in voxels, the ventilated volume, the
16
17 minimum, mean, modal, median and maximum grey values, IOD, contrast, histogram, and
18
19 Kurtosis on a per-ROI basis. Mean values weighted by ROI area were calculated for left,
20
21 right, and total lung.

22
23
24
25
26 A voxel was considered to represent ventilated lung tissue if it had a grey value larger than
27
28 20% of the histogram maximum. To minimise the impact of any erratic hot pixels, the
29
30 histogram maximum was calculated from the 97% level assuming that the histogram above
31
32 97% drops with a slope of -0.5. In this work we only report the results for total lungs, but it is
33
34 noted that the software reports more details where this may be of interest.

35
36
37
38
39 The second step of the analysis created 8-bit grey-level co-occurrence matrices (GLCMs)
40
41 from all the ROIs of any one lung for 5 distances each: 1, 2, 4, 8, and 12 pixels (4.7, 9.3, 18.7,
42
43 37.3, 56.0mm) and for 4 direction pairs each: X (left->right, right->left), Y (top->bottom,
44
45 bottom->top), Z (up->down, down->up) and I (invariant, combining X, Y, and Z). The
46
47 invariant matrix we chose gives equal weight to each valid voxel pair and may at times differ
48
49 from a mean over the X, Y, and Z matrices as individual matrices may not have the exact
50
51 same number of voxel pairs. From these GLCMs twelve texture features were calculated as
52
53 listed in appendix A (Haralick *et al.*, 1973, Haralick 1979, Choi, 1996).
54
55
56
57
58
59
60
61
62
63
64
65

3. Results

3.1 Results from the phantom study

The texture parameters calculated from the simulated lungs show a number of correlations with the size of the defects and the total non-ventilated volume (NVV). Figure 1 illustrates this for the example of the textural parameter TC18 (coefficient of variation) and simulated defect sizes of 3x3x3 pixels. For all GLCM distances and defect sizes the parameter TC18 increases steadily with increasing NVV and more rapidly so for larger defects.

No significant differences were found between results obtained from X, Y, and Z GLCMs.

Hence only the invariant GLCMs have been studied further. For all 12 textural parameters studied we found under all conditions that the functions such as in Figure 1 are smooth and steady and that different distances in GLCM calculation result in slightly shifted versions of the same shape but that in no case does the graph of one distance cross the graph of another distance for otherwise identical settings. On the contrary, we often saw that graphs for different distances were almost undistinguishable from one another. Consequently the data from all distances were pooled into one; thus reducing the complexity of the results presented. Notwithstanding this, it is noted, that TC9 and TC30 were somewhat more sensitive to NVV changes at shorter distances and that TC2 showed no dependence on NVV but gave significantly different results for different distances.

For clarity only the relative changes in textural parameters between the lowest and highest NVV studied are reported, because the functions change smoothly with NVV and in-between values do not add much to the discussion.

Table 1 lists the relative changes in the textural parameters calculated in response to a 40% drop in ventilated lung volume. Some textural parameters are more sensitive to the changes in ventilated volume than others as can be seen from Table 1 (rows 6 and 11 “*mean*”). Also,

1 they are typically stronger in the contrast-stretched data set (*cs*, row 6) as compared to the
2
3 histogram-matched data set (*hm*, row 11).
4
5

6 The results from a sensitivity test to brightness changes are shown in Table 2. We repeated the
7
8 simulation for the “worst” lung with a higher activity such that after adding the defects it
9
10 resulted in the same IOD as the perfectly ventilated simulated lung. Insensitivity to brightness
11
12 changes would allow the direct comparison of textural parameters derived from studies that
13
14 use different gamma counts. Note that rows 2 and 3 in Table 2 correspond to rows 5 and 10 in
15
16 Table 1 (10 mm), respectively, but the percentage changes are expressed relative to the values
17
18 in Table 1. It is noted that the sign of all values in Table 2 act in such a way as to reduce the
19
20 sensitivity of the textural parameters.
21
22
23
24
25

26 In the context of our work a good textural parameter is one that is sensitive to changes in
27
28 NVV or defect-size and that is at the same time insensitive to changes in brightness. With this
29
30 in mind we can group the textural parameters investigated into robust, intermediate and poor
31
32 performers:
33
34
35
36
37
38
39

40 **Robust textural parameters:**

41
42 TC13/TC31 Variance/Mean ratio: provides a solid signal of 22% change in the parameter
43
44 value for a 40% change in NVV while its dependence on brightness doubling is only small
45
46 (1.5%). The sensitivity is somewhat poorer for smaller defects.
47
48
49

50 TC30 Local homogeneity: provides still a good signal of 10.5% change for a 40% drop in
51
52 NVV but is more sensitive to brightness changes than the TC13/TC31 ratio (2.9%).
53
54
55

56 TC18 Coefficient of Variation: provides a very strong signal of 77% for large defects and a
57
58 still strong signal of 22% for small defects. It has a moderate dependence on brightness
59
60 changes (10.8% simulating large defects). However, correlation with clinical data discussed
61
62
63
64
65

1 below is excellent.
 2
 3
 4
 5
 6

7 **Textural parameters with intermediate performance:**
 8

9
 10 TC1 Angular second moment: provides high sensitivity (>68%) to changes in NVV, but
 11
 12 unfortunately it is also very sensitive to brightness changes.
 13
 14

15 TC2 and TC2: Difference and inverse difference moment: show a modest sensitivity for short
 16
 17 distances and small-sized defects but are insensitive at larger pixel distances as well as for
 18
 19 larger defect sizes. However, they may be used successfully in conjunction with other
 20
 21 parameters to decide whether the effective size distribution of the non-ventilated volumes is
 22
 23 small or large.
 24
 25

26
 27 TC9 Correlation: The theoretical study shows a reasonable sensitivity of around 20% to
 28
 29 changes twice that large in NVV but also a relatively high sensitivity to brightness changes. In
 30
 31 the clinical studies discussed below this parameter did not convince and is outperformed by
 32
 33 others.
 34
 35
 36
 37
 38
 39
 40

41 **Textural parameters with poor performance:**
 42

43
 44 TC7, TC4, TC13, TC31, TC21, and TC23: These parameters suffer either from a lack of
 45
 46 sensitivity or high sensitivity to changes in brightness.
 47
 48
 49
 50
 51

52 **Combination of textural parameters:**
 53

54
 55 The ratio of TC13/TC31 is a very good performer although neither TC13 nor TC31 are good
 56
 57 performers. Similarly, the ratio of TC21/TC31 gives a moderately good performance.
 58
 59
 60
 61
 62
 63
 64
 65

3.2 Results from the clinical studies

Figure 2 illustrates the estimated ventilated lung volume grouped by patient group. The 'normal' group shows the highest ventilated volume of about 90% and the smallest variance. Asthmatic lungs at baseline show a slightly lower ventilated lung volume although not statistically significant from the 'normal' lungs. The remaining patient groups show significant reductions in ventilated lung volume that are strongest in COPD patients. There is also a higher variability in these groups.

Figures 3 and 4 illustrate one of the best performing textural parameters for the 5 patient groups studied. Both the absolute value and the variability between different GLCM distances and between patients in the 'normal' lung function group are small (Figure 3, left panel). The results from COPD patients which range from a mild case (right panel, c-01) to severe (c-05) show increasingly higher values.

The differences between using different distances in the GLCM calculations are almost within the numerical precision, which was also observed in the results from the simulated data. This observation holds true for all textural parameters and patient groups studied except for TC2, TC9 and TC30. TC9 (Correlation) and TC30 (Local Homogeneity) lose sensitivity with increasing distance between voxel pairs and better performance is achieved by only using the 2 shortest distances (1 and 2 pixels distance corresponding to 4.7 and 9.3mm, respectively). TC2 will be discussed separately below. These findings are consistent with observations from the simulated data.

Pooling the data from all GLCM distances² and by patient group allows us to look for disease-specific differences as shown in Figure 4. While asthmatics at baseline cannot be distinguished from normal lungs, they can be clearly identified after a Metacholine challenge. PELICAN patients and even more so COPD patients have strongly elevated values in the coefficient of

² Except for TC9 and TC30 which pooled only the 2 shortest distances for higher sensitivity

1 variation calculated from the GLCM.

2
3
4 Figure 5 presents the ratio of Local Homogeneity and GLCM Mean (TC30/TC31) calculated
5
6 in the same way as in the previous figure. Again, values for COPD and PELICAN patients are
7
8 significantly higher than those for normal and asthmatic lungs. It is noted, however, that
9
10 asthma patients both at baseline and at Metacholine challenge give almost identical results.
11
12 Hence combining the information from multiple textural parameters allows to distinguish
13
14 between different disease classes such as asthma from COPD.
15
16

17
18
19 A very strong correlation ($r^2=0.955$) between the textural parameter Coefficient of Variation
20
21 (TC18) and the estimated ventilated lung volume is illustrated in Figure 6. Similarly high
22
23 correlations of $r^2>0.8$ exist for textural parameters TC3, TC30, TC31, and the ratios
24
25 TC13/TC31 and TC21/TC31 as a function of ventilated lung volume (not illustrated). More
26
27 positive correlations ($r^2>0.49$) are observed for textural parameters TC1, TC9, and the ratio
28
29 TC1/TC31.
30
31

32
33
34 Independent spirometry data in the form of the predicted forced expiratory volume during 1
35
36 second (FeV1) was available for all but the 'normal' group. Again good correlations are
37
38 observed with several textural parameters ($r^2>0.5$ for TC18 and TC13/TC31, $r^2>0.4$ for TC3,
39
40 TC30, TC21/TC31, TC31 and TC1/TC31 and $r^2>0.3$ for TC1, TC2 and TC9) as illustrated in
41
42 Figure 7 for the example of TC13/TC31.
43
44

45
46 The Difference Moment (TC2) behaves differently from all other textural parameters studied.
47
48 It is insensitive to changes in both NVV and FeV1, but it is sensitive to the size distribution of
49
50 patterns in the lung. Hence the TC2 textural parameter results were prepared in a different
51
52 way. Instead of pooling the results from different GLCM distances, the parameter value
53
54 obtained with the shortest distance (1 pixel) were divided by the parameter value for the
55
56 second largest distance for any one lung and that we refer to as TC2_d for short. Data prepared
57
58 in this way resulted in a positive correlation of TC2_d with NVV ($r^2=0.69$) and a somewhat
59
60
61
62
63
64
65

1 weaker correlation with FeV1 ($r^2=0.375$).
2
3

4 All results in this section were derived from the contrast-stretched data set as it showed an
5 overall better performance than compared to results derived from the histogram-matched data.
6
7

8 It is noted that TC18, TC31 (Mean) and TC13/TC31 were indifferent to both NVV and FeV1
9 changes in the histogram-matched data set, but otherwise the same textural parameters
10 performed well as in the contrast-stretched data set. The only textural parameter that faired
11 significantly better in the histogram-matched data set was TC23 (Difference Entropy).
12
13
14
15
16
17
18
19
20
21

22 **4 Discussion**

23
24

25 Changes in the grey level distribution such as a shift to darker grey values – as can be
26 expected with a reduction in ventilated lung volume – is essentially removed in the histogram-
27 matched data. Hence, changes in the textural parameters that occur in the contrast-stretched
28 data set but not in the histogram-matched one are thought to be driven by histogram changes
29 while changes that occur in the histogram-matched data set are thought to be dominated by
30 changes in pattern (Table 1). Changes in the contrast-stretched data set are often a result of
31 both histogram and pattern changes.
32
33
34
35
36
37
38
39
40
41

42 In an ideal system a change in brightness should not affect the textural parameters calculated
43 because the GLCMs are always normalised to an IOD of unity. However, it is noted that the
44 spatial resolution of the observation system is significantly lower than the features that cause
45 them. The effective resolution in the SPECT-V data is lower than the pixel resolution of
46 4.664mm/pxl which in turn is much coarser than the simulated small defects starting from
47 2.5mm cube side length. Due to the nature of discrete sampling – and in this case significant
48 under-sampling – of the object space and the non-linearity of the resulting effective blurring,
49 the texture parameters calculated become dependent on the total optical density and contrast
50
51
52
53
54
55
56
57
58
59
60
61
62
63
64
65

1 in the SPECT-V data sets. This effect itself is also dependent on the effective size distribution
2
3 of the defects we seek to describe. To quantitatively describe the exact relationship is
4
5 mathematically complex and of limited practical use as it will vary from situation to situation.
6
7 Instead we seek to identify textural parameters that depend acceptably little on the variability
8
9 in patient data preparation.
10
11

12
13 The simulated data allows to fully control the environment, to know the true size distribution
14
15 of the non-ventilated lung volumes, the true ventilated volume, and to vary some of these
16
17 parameters systematically to study its impact. However, there are also some differences and
18
19 limitations compared to clinical data that are undesirable. One is that the IOD of the simulated
20
21 SPECT-V scan drops progressively with increasing NVV due to the simplicity of the model
22
23 available to us.
24
25

26
27 A patient with a smaller ventilated lung volume inhales approximately the same amount of
28
29 radioactivity as a patient with a larger ventilated lung volume. As a result the scan from the
30
31 former patient would have a larger information content³ and image contrast; because the same
32
33 amount of activity has to squeeze into a smaller volume, a wider range of different brightness
34
35 values is observed. Hence a poorly ventilated *simulated* lung has a somewhat *lower*
36
37 information content in the simulated data in contrast to a patient with a poorly ventilated lung
38
39 that would result in a *higher* information content than the ideally ventilated lung. We studied
40
41 this behaviour by simulating one data set with a higher gamma count, which resulted in an
42
43 increase of 38% in information content as opposed to a 9% drop in the non-corrected
44
45 simulation case. Although the textural parameters are modified as a result, it does not change
46
47 the overall response to NVV and we were able to identify textural parameters that are little or
48
49 non-susceptible to this change (Table 2). This finding is also directly relevant to clinical data,
50
51 because any two patients with naturally differently-sized lungs that are administered the same
52
53
54
55
56
57
58
59

60 ³ We use the term information content in the strict sense of the number of grey values in an associated
61 histogram that are non-zero.
62
63
64
65

1 amount of Technegas will have differences in contrast and information content of the SPECT
2
3 recorded. Selecting textural parameters that are insensitive to this variability in data collection
4
5 is an advantage in data interpretation.
6

7
8 Reconstructed SPECT data is routinely subjected to a rather strong smoothing filter before
9
10 being presented to a radiographer or other medical professional. Filtering at the RNSH
11
12 consists of a 9th order Butterworth filter with a cut-off of 1.2 cycles per centimetre. Since
13
14 texture analysis by definition looks at small differences in grey values between pairs of pixels,
15
16 any smoothing operation degrades the capabilities of the method for any given case. We tested
17
18 this expected behaviour by preparing both simulated and normal patient data with and
19
20 without applying the Butterworth filter and found the smoothed data set to have a poorer
21
22 sensitivity as manifested in smaller relative changes in textural parameters. We will report the
23
24 exact impact in a forthcoming separate study. In this work we only discuss reconstructed,
25
26 extracted lung data that has **not** been subjected to any post-filtering.
27
28
29
30
31

32
33 A change of distance in the calculation of the GLCMs (within reason) adds little new
34
35 information (Figure 1) with the exception of parameter TC2. In most cases the calculation of
36
37 the GLCM for only one distance seems to be sufficient. For 2 of the textural parameters
38
39 studied there is a better performance seen for shorter distances in the GLCM calculations
40
41 (TC9 and TC30). This is plausible looking at the definitions (Appendix 1). Voxel pairs that are
42
43 far from one another are unlikely to be highly correlated thus giving low correlation values in
44
45 any lung (TC9) and uniformity between them will be near the random value (TC30).
46
47
48
49

50
51 From the simulated data it is known that TC2_d drops with increasing defect size and in the
52
53 patient data it drops with increasing NVV. This suggests that the average size of individual,
54
55 non-ventilated areas increases with the severity of the diseases studied as opposed to a mere
56
57 increase of number of non-ventilated areas of same size. This result is consistent with the
58
59 perception of the SPECT data to the human eye.
60
61
62
63
64
65

1 Several well performing textural parameters were identified that by themselves allow to
2 distinguish between a 'normal' lung and a lung that suffers from some significant medical
3 condition or disease. Combinations of textural parameters have the potential to further
4 classify abnormal lungs. For example, to distinguish between asthmatics on one hand and
5 COPD patients on the other hand one can combine the results from TC18 and the ratio
6 TC30/TC31. TC18 is elevated in all diseases, but the ratio TC30/TC31 does not rise
7 significantly in asthmatics while it does rise significantly in COPD patients (compare Figures
8 4 and 5).

9
10
11
12
13
14
15
16
17
18
19
20
21 Correlation of several key textural parameters with the corresponding ventilated lung volume
22 are good to excellent for all patient data (Figures 6 and 7). Note that the ventilated lung
23 volume is a measure that is calculated from the original imaging data (not the GLCM), while
24 the FeV1 is a completely independent measurement. The pooling of data per disease group
25 (Figures 4 and 5) combines all patients of one disease into one - independent of the severity of
26 disease. Figures 6 and 7 on the other hand illustrate the relationship between reduced lung
27 functionality and resulting changes in derived textural parameters. It is pointed out that
28 reduced lung functionality goes along with higher heterogeneity in the SPECT data (Berend *et*
29 *al.*, 2008) and textural parameters that measure heterogeneity increase while parameters that
30 measure uniformity drop.

31
32
33
34
35
36
37
38
39
40
41
42
43
44
45
46 The textural parameters discussed are not all linearly independent of one another but some of
47 them have substantial correlations amongst them. (Clausi, 2008). For practical matters it is
48 desirable to identify a small number of textural parameters that give the overall best
49 classification performance.

50
51
52
53
54
55
56
57
58
59
60
61
62
63
64
65
66
67
68
69
70
71
72
73
74
75
76
77
78
79
80
81
82
83
84
85
86
87
88
89
90
91
92
93
94
95
96
97
98
99
100
101
102
103
104
105
106
107
108
109
110
111
112
113
114
115
116
117
118
119
120
121
122
123
124
125
126
127
128
129
130
131
132
133
134
135
136
137
138
139
140
141
142
143
144
145
146
147
148
149
150
151
152
153
154
155
156
157
158
159
160
161
162
163
164
165
166
167
168
169
170
171
172
173
174
175
176
177
178
179
180
181
182
183
184
185
186
187
188
189
190
191
192
193
194
195
196
197
198
199
200
201
202
203
204
205
206
207
208
209
210
211
212
213
214
215
216
217
218
219
220
221
222
223
224
225
226
227
228
229
230
231
232
233
234
235
236
237
238
239
240
241
242
243
244
245
246
247
248
249
250
251
252
253
254
255
256
257
258
259
260
261
262
263
264
265
266
267
268
269
270
271
272
273
274
275
276
277
278
279
280
281
282
283
284
285
286
287
288
289
290
291
292
293
294
295
296
297
298
299
300
301
302
303
304
305
306
307
308
309
310
311
312
313
314
315
316
317
318
319
320
321
322
323
324
325
326
327
328
329
330
331
332
333
334
335
336
337
338
339
340
341
342
343
344
345
346
347
348
349
350
351
352
353
354
355
356
357
358
359
360
361
362
363
364
365
366
367
368
369
370
371
372
373
374
375
376
377
378
379
380
381
382
383
384
385
386
387
388
389
390
391
392
393
394
395
396
397
398
399
400
401
402
403
404
405
406
407
408
409
410
411
412
413
414
415
416
417
418
419
420
421
422
423
424
425
426
427
428
429
430
431
432
433
434
435
436
437
438
439
440
441
442
443
444
445
446
447
448
449
450
451
452
453
454
455
456
457
458
459
460
461
462
463
464
465
466
467
468
469
470
471
472
473
474
475
476
477
478
479
480
481
482
483
484
485
486
487
488
489
490
491
492
493
494
495
496
497
498
499
500
501
502
503
504
505
506
507
508
509
510
511
512
513
514
515
516
517
518
519
520
521
522
523
524
525
526
527
528
529
530
531
532
533
534
535
536
537
538
539
540
541
542
543
544
545
546
547
548
549
550
551
552
553
554
555
556
557
558
559
560
561
562
563
564
565
566
567
568
569
570
571
572
573
574
575
576
577
578
579
580
581
582
583
584
585
586
587
588
589
590
591
592
593
594
595
596
597
598
599
600
601
602
603
604
605
606
607
608
609
610
611
612
613
614
615
616
617
618
619
620
621
622
623
624
625
626
627
628
629
630
631
632
633
634
635
636
637
638
639
640
641
642
643
644
645
646
647
648
649
650
651
652
653
654
655
656
657
658
659
660
661
662
663
664
665
666
667
668
669
670
671
672
673
674
675
676
677
678
679
680
681
682
683
684
685
686
687
688
689
690
691
692
693
694
695
696
697
698
699
700
701
702
703
704
705
706
707
708
709
710
711
712
713
714
715
716
717
718
719
720
721
722
723
724
725
726
727
728
729
730
731
732
733
734
735
736
737
738
739
740
741
742
743
744
745
746
747
748
749
750
751
752
753
754
755
756
757
758
759
760
761
762
763
764
765
766
767
768
769
770
771
772
773
774
775
776
777
778
779
780
781
782
783
784
785
786
787
788
789
790
791
792
793
794
795
796
797
798
799
800
801
802
803
804
805
806
807
808
809
810
811
812
813
814
815
816
817
818
819
820
821
822
823
824
825
826
827
828
829
830
831
832
833
834
835
836
837
838
839
840
841
842
843
844
845
846
847
848
849
850
851
852
853
854
855
856
857
858
859
860
861
862
863
864
865
866
867
868
869
870
871
872
873
874
875
876
877
878
879
880
881
882
883
884
885
886
887
888
889
890
891
892
893
894
895
896
897
898
899
900
901
902
903
904
905
906
907
908
909
910
911
912
913
914
915
916
917
918
919
920
921
922
923
924
925
926
927
928
929
930
931
932
933
934
935
936
937
938
939
940
941
942
943
944
945
946
947
948
949
950
951
952
953
954
955
956
957
958
959
960
961
962
963
964
965
966
967
968
969
970
971
972
973
974
975
976
977
978
979
980
981
982
983
984
985
986
987
988
989
990
991
992
993
994
995
996
997
998
999
1000

1 recommend for use. As TC3 and TC30 are highly correlated one should choose only one of
2
3 them with TC3 performing marginally better in contrast-stretched data sets and TC30 better in
4
5 histogram-matched data sets.
6

7
8 TC1, TC21 and TC23 are all measures of orderliness. The ratio TC21/TC31 performed best in
9
10 the clinical data. The GLCM Mean (TC31) reflects brightness changes between patients that
11
12 the contrast-stretched data set is susceptible to. Thus using textural parameter combinations
13
14 that involve the GLCM Mean improves correlation in several textural parameters studied. The
15
16 histogram-matched data set shows no correlation with TC31 and combining textural
17
18 parameters with TC31 carries no advantage and TC23 by itself gives the best performance in
19
20 the group of textural parameters that measure orderliness. The value of Entropy (TC21, TC23)
21
22 increases with increasing heterogeneity.
23
24
25
26

27
28 TC9 (Correlation), TC13 (Variance), TC18 (Coefficient of Variation) and TC31 (Mean) are
29
30 descriptive statistics of the GLCMs and the frequency at which certain voxel *pairs* occur. The
31
32 combination of Variance and Mean in the Coefficient of Variation (TC18) and the Variance
33
34 over Mean ratio (TC13/TC31) gave excellent performance in the contrast-stretched data set
35
36 and is another recommended parameter for use. TC18 and the TC13/TC31 ratio are highly
37
38 correlated parameters. TC18 shows better correlation with ventilated lung volume and
39
40 TC13/TC31 shows better correlation with FeV1 but either one being a very good choice for
41
42 characterising the clinical data.
43
44
45
46

47
48 GLCM Correlation (TC9) Is largely independent of the other texture measures and has the
49
50 potential for giving additional insight. TC9 can be calculated for increasingly larger voxel
51
52 distances and the size at which the value suddenly decreases is a measure for the size of
53
54 definable objects in the original image data. However, we could not identify any 'sharp' drops
55
56 but only gradual changes with the clinical data, suggesting that there is a broad size
57
58 distribution of objects which makes this approach less powerful. Simply comparing the
59
60
61
62
63
64
65

1 differences in Correlation values between the shortest and longest distance studied with
2 ventilated lung volume resulted in a modest correlation ($r^2=0.41$).
3
4

5
6 It is noted that the best correlations between textural parameters and ventilated lung volume
7 were achieved with a linear regression while correlation with FeV1 gave consistently better
8 results using a logarithmic correlation function.
9

10 Summed up the following 3 recommendations can be made for the analysis of pulmonary
11 SPECT-V data.
12
13

- 14 1) Texture analysis sensitivity is maximised by preparing SPECT data in an unfiltered,
15 contrast-stretched way, as opposed to filtered or histogram-matched.
16
17
- 18 2) The choice of voxel pair distance in the GLCM calculation is non-critical. With
19 present spatial resolution in SPECT data 1, 2, or 3 pixel distances are good choices
20 that can also be pooled to improve statistics.
21
22
- 23 3) Amongst the many textural parameters studied one each should be chosen from 3
24 different groups of parameters to balance the capability to characterise with the
25 computational effort involved. These are the textural parameters TC18 or the ratio
26 TC13/TC31 from the descriptive statistics group, the parameter TC3 or TC30 from the
27 contrast group and the parameter ratio TC21/TC31 in the orderliness group.
28
29
30
31
32
33
34
35
36
37
38
39
40
41
42
43
44

45 Application of the new software package is not limited to pulmonary studies – in fact it may
46 also be applied to other organs or to completely different fields such as material sciences or
47 mineralogy. However, in its present form the software package is optimized to the work-flow
48 of studying lungs in a clinical scenario.
49
50
51
52
53

54 55 56 57 58 59 **Summary** 60 61 62 63 64 65

1 It has been demonstrated that a textural parameter analysis of functional pulmonary CT data
2
3 has the potential to provide a robust and objective quantitative characterisation of
4
5 inhomogeneity in lung function and classification of lung diseases with application in routine
6
7 clinical applications and national screening programmes. The new methods applied to SPECT
8
9 lung ventilation scans are capable of distinguishing between different types of diseases.
10
11 Strong correlations between key textural parameters and independent lung function data such
12
13 as the FeV1 suggest that a quantitative description of the severity of diseases such as asthma
14
15 or COPD by means of derived texture parameters is viable. Clear recommendations have been
16
17 made for optimum data preparation and textural parameter selection. In a forthcoming study
18
19 we plan to use data from larger numbers of patients and additional spirometry data to further
20
21 refine the methods.
22
23
24
25
26
27
28
29
30

31 **Acknowledgements**

32
33 This work is supported by the Australian Research Council through the ARC Linkage Project
34
35 LP0562715. The authors are grateful for scientific and technical input and support from the
36
37 Australian Microscopy & Microanalysis Research Facility (AMMRF) node at
38
39 the University of Sydney. We also like to thank the staff at the Royal North Shore Hospital
40
41 that helped in the data collection and the volunteer patients that participated in this study. In
42
43 particular we like to thank Peter Chicco, Department of Biomedical Engineering, who
44
45 provided the lung simulations, Dale and Elizabeth Bailey, Department of Nuclear Medicine,
46
47 for discussion and data conversion.
48
49
50
51
52
53

54 We like to thank Wayne Rasband and all other developers that made contributions to ImageJ
55
56 and its plug-ins for sharing their work freely with other researchers (Rasband, 1997-2008,
57
58 Abramoff *et al.*, 2004) – without them our work would have been much harder. Part of the
59
60
61
62
63
64
65

software presented here started their development based on other publicly available plug-ins that are accessible through the ImageJ web page (Rasband,1997-2008, Castleman, 2005, Miller, 2002).

References

- Abramoff, MD, Magelhaes, PJ, Ram, SJ, Image Processing with ImageJ, Biophotonics International (2004), **11**(7):36-42
- Berend N, Salome CM, King GG, Mechanisms of airway hyper-responsiveness in asthma. *Respirology* (2008), **13**(5):624-631
- Burger W and Burge MJ, Digital Image Processing - An Algorithmic Approach using Java. Springer-Verlag, New York (2008). ISBN 978-1-84628-379-6, www.imagingbook.com
- Cabrera JE, “GLCM_Texture” plug-in for ImageJ, (2005), <http://rsb.info.nih.gov/ij/plugins/>
- Castleman M, “Cell_outliner” plug-in for ImageJ (m@mlcastle.net), Columbia University (2005) <http://rsb.info.nih.gov/ij/plugins/cell-outliner.html>
- Chicco P, Magnussen JS, Mackey DW, Bush V, Emmett L, Storey G, Bautovich G, and Wall H van der, SPET of a computerised model of diffuse lung disease, *Eur.J.Nuc.Med* (2001), **28**(2):150-154
- Choi HK, New Methods for Image Analysis of Tissue Sections. PhD thesis, Uppsala University, Sweden (1996), ISBN 91-554-3829-6
- Clausi DA, An analysis of co-occurrence texture statistics as a function of grey level quantization. *Can. J. Remote Sensing*, (2002), **28**(1):45–62
- Craddock TD, Bailey DL, Hutton BF, Conninck F De, Busemann-Sokole E, Bergmann H, and Noelpp U, A standard protocol for the exchange of nuclear medicine image files. *NucMedComm* (1989), **10**:703-713
- Downie SR, Salome CM, Verbanck S, Thompson BR, Berend N and King GG, Ventilation heterogeneity is a major determinant of airway hyperresponsiveness in asthma, independent of airway inflammation. *Thorax* (2007), **62**:684-689
- Haralick RM, Shanmugam K, and Dinstein I, Textural features for image classification. *IEEE Transactions on Systems, Man, and Cybernetics* (1973), **SMC-3**(6):610-621
- Haralick RM, Statistical and structural approaches to texture. *Proceedings of the IEEE* 67 (1979), **5**:786-804
- Harris BE, Bailey D, Miles S, Bailey E, Rogers K, Roach P, Thomas P, Hensley M, and King GG, “Objective analysis of tomographic ventilation perfusion scintigraphy in pulmonary embolism”, *Am. J. Respir. Crit. Care Med.* , March 15, 2007
- Haynor DR, Harrison RL, Lewellen TK, The use of importance sampling techniques to improve the efficiency of photon tracking in emission tomography simulations. *Med Phys* (1991), **18**:990–1001
- King GG, Eberl S, Salome CM, Meikle SR, and Woolcock AJ, Airway closure measured by a Technegas bolus and SPECT. *Am.J.Respir.Crit.CareMed.* (1997) **155**:682–688

- 1 King GG, Eberl S, Salome CM, Young IH, and Woolcock AJ, Differences in airway closure
 2 between normal and asthmatic subjects measured with single-photon emission computed
 3 tomography and technegas. *Am.J.Respir.Crit.CareMed.* (1998), **158**:1900–1906.
 4
- 5 Lewellen TK, Anson CP, Haynor DR, Design of a simulation system for emission
 6 tomographs. *J Nucl Med* (1988), **29**:871
 7
- 8 Miller M, “Segmenting_Assistant”, plug-in for ImageJ, (2002) mmiller3@iupui.edu,
 9 <http://rsb.info.nih.gov/ij/plugins/index.html>
 10
- 11 Parker JA, Align3_TP: stack alignment plug-in for ImageJ, J.A.Parker@IEEE.org (version
 12 25/Mar/2008), <http://www.med.harvard.edu/JPNM/ij/plugins/Align3TP.html>
 13
- 14 Petersson J, Sánchez-Crespo A, Larsson SA and Mure M, Physiological imaging of the lung:
 15 single-photon-emission computed tomography (SPECT). *J Appl Physiol* (2007) **102**:468-476
 16
- 17 Rasband, W.S., ImageJ, U. S. National Institutes of Health, Bethesda, Maryland, USA,
 18 <http://rsb.info.nih.gov/ij/>, 1997-2008.
 19
- 20 Tgavalekos NT, Musch G, Harris RS, Vidal Melo MF, Winkler T, Schroeder T, Callahan R,
 21 Lutchen KR and Venegas JG, Relationship between airway narrowing, patchy ventilation and
 22 lung mechanics. *Eur Respir J* (2007), **29**:1174–1181
 23
- 24 Venegas JG, Schroeder T, Harris S, Winkler RT, and Vidal Melo MF, The distribution of
 25 ventilation during bronchoconstriction is patchy and bimodal: A PET imaging study.
 26 *Respiratory Physiology & Neurobiology* (2005) **148**:57–64
 27
- 28 WHO World Health Organisation, 2008a, <http://www.who.int/respiratory/asthma/en/>
 29
- 30 WHO World Health Organisation, 2008b, <http://www.who.int/respiratory/copd/en/>
 31
- 32 Xu J, Moonen M, Johansson Å, Gustafsson A, and Bake B, Quantitative analysis of
 33 inhomogeneity in ventilation SPET. *Eur J Nucl Med* (2001) **28**:1795–1800
 34
- 35 Zubal IG, Harrell CR, Smith EO, Rattner Z, Gindi G, Hoffer PB, Computerized three-
 36 dimensional segmented human anatomy. *Med Phys* (1994), **21**:299–302
 37
 38
 39
 40
 41
 42
 43
 44
 45
 46
 47
 48
 49
 50
 51
 52
 53
 54
 55
 56
 57
 58
 59
 60
 61
 62
 63
 64
 65

Appendix A: Definition of textural features from the co-occurrence matrix

A co-occurrence matrix $P(i,j|d,\theta)$ (PM for short) contains the probability that the grey level i occurs at a distance d in direction θ from a pixel with grey value j . N is the size of the co-occurrence matrix ($N=256$ in this study). Integrated sums are calculated from the matrix variance. We further define the vertical ($p_x(i)$), horizontal ($p_y(i)$), minor diagonal ($p_{x-y}(k)$) sums, the vertical (μ_x) and horizontal (μ_y) mean, and the variance of the vertical (V_x) and horizontal (V_y) directions (Choi, 1996). Note that the GLCM mean is distinct from the mean grey value of the original image because it is weighted by the frequency of occurrence *in combination with* a certain neighbour pixel value.

$$P_x[i] = \sum_{j=0}^{N-1} PM, \quad P_y[j] = \sum_{i=0}^{N-1} PM, \quad P_{x-y}[k] = \sum_{i=0, i+j=k}^{N-1} \sum_{j=0}^{N-1} PM, \quad \mu_x = \sum_i i P_x[i],$$

$$\mu_y = \sum_j j P_y[j], \quad V_x = \sum_i [i - \mu_x]^2 P_x[i], \quad V_y = \sum_j [j - \mu_y]^2 P_y[j]$$

TC_1 Angular Second Moment $\sum_{i=0}^{N-1} \sum_{j=0}^{N-1} PM^2$

TC_2 Difference Moment or GLCM Contrast $\sum_{i=0}^{N-1} \sum_{j=0}^{N-1} [i - j]^2 PM$

TC_3 Inverse Difference Moment, $\sum_{i=0}^{N-1} \sum_{j=0}^{N-1} \frac{1}{|i - j|^2} PM$

TC_4 Diagonal Moment, $\sum_{i=0}^{N-1} \sum_{j=0}^{N-1} \frac{1}{|0.5[i - j]|} PM$

TC_7 Inertia, $\sum_{n=0}^{N-1} n^2 \sum_{i=0, i-j=n}^{N-1} \sum_{j=0}^{N-1} [i - j]^2 PM$

TC_9 GLCM Correlation, $\frac{\sum_{i=0}^{N-1} \sum_{j=0}^{N-1} ij PM - \mu_x \mu_y}{\sqrt{V_x V_y}}$

TC13 GLCM Variance, V_x

TC18 Coefficient of Variation, $\frac{\sqrt{V_x V_y}}{\mu_x \mu_y}$

TC21 Entropy, $\sum_{i=0}^{N-1} \sum_{j=0}^{N-1} PM \ln PM$

TC23 Difference Entropy, $\sum_{i=0}^{N-1} P_{x-y}[i] \log_e P_{x-y}[i]$

TC30 Local Homogeneity, $\sum_{n=0}^{N-1} \frac{1}{|n|+1+n^2}$

TC31 GLCM Mean $0.5[\mu_x + \mu_y]$

histogram	cube side length [mm]	TC_1 Angular Second Moment	TC_3 Inverse Different Moment	TC_4 Diagonal Moment	TC_9 Correlation	TC18 Coefficient of Variation	TC21 Entropy	TC30 Local Homogeneity	TC13 Sum of squares / Variance	TC31 Mean	TC13/TC31 Variance / Mean ratio
cs	2.5	111.9	4.2	-27.1	-15.2	22.5	-8.4	4.2	-2.2	-10.6	9.5
cs	5.0	106.4	7.5	-27.3	-20.0	28.9	-8.0	7.5	-16.8	-19.6	3.5
cs	7.5	85.8	9.0	-23.3	-22.3	46.6	-6.7	9.0	-17.7	-25.1	9.8
cs	10.0	68.6	10.5	-20.2	-19.2	77.0	-5.6	10.5	-15.6	-30.9	22.2
cs	mean	93.2	7.8	-24.5	-19.2	43.7	-7.2	7.8	-13.1	-21.6	11.3
hm	2.5	111.9	2.3	-27.2	-11.7	-0.7	-8.4	2.3	-0.4	0.1	-0.6
hm	5.0	106.4	-0.4	-24.9	-15.6	-0.1	-8.0	-0.4	-0.3	-0.1	-0.2
hm	7.5	85.8	0.4	-21.5	-16.1	-1.0	-6.8	0.4	-1.3	-0.2	-1.1
hm	10.0	68.6	2.1	-18.7	-13.8	0.1	-5.6	2.1	-1.1	-0.6	-0.5
hm	mean	93.2	1.1	-23.1	-14.3	-0.4	-7.2	1.1	-0.8	-0.2	-0.6

Table 1: Sensitivity of textural parameters to a 40% reduction in ventilated lung volume. The latter was achieved by randomly inserting black cubes of side length 2.5, 5, 7.5 and 10mm into the simulated lung. Results are shown as relative changes in the textural parameter for either preparing the data in a histogram-matched (hm) or a contrast-stretched (cs) way and as a mean over 5 distances used in the GLCM calculation.

Histogram	TC 1 Angular Second Moment	TC 3 Inverse Different Moment	TC 4 Diagonal Moment	TC 9 Corre lation	TC18 Coefficient of Variation	TC21 Entro py	TC30 Local Homog eneity	TC13 Sum of squares (Variance)	TC31 Mean	TC13/ TC31 Variance /Mean ratio
cs	-62.6	-2.9	53.4	10.8	-10.8	11.5	-2.9	8.7	10.4	-1.5
hm	-62.3	-3.9	48.5	9.0	0.5	11.3	-3.9	-0.1	-0.3	0.2

Table 2: Sensitivity of textural parameters to a 40% increase in gamma counts. The simulated defects have a cube side length of 10mm. Listed are the differences in the values of the textural parameters derived from either the standard simulation with 40% NVV and associated drop in average brightness and an alternative simulation with a higher gamma count such that after knocking out 40% of the ventilated volume the IOD matched the IOD of the perfectly ventilated lung simulation.

Figure captions

Figure 1: Illustration of textural parameter TC18, Coefficient of Variation, from the simulation study for cube-shaped defects of size 7.5mm cube side length as a function of non-ventilated lung volume in percent. The GLCMs were created for 5 pixel distances each (1, 2, 4, 8, 12 pixels) corresponding to distances in the lung of 4.7, 9.3, 18.7, 37.3 and 56.0mm, respectively. The coefficient of variation is larger for small pixel distances and increases with NVV and more rapidly so for larger defects (not illustrated).

Figure 2: Relative ventilated lung volume (solid black) and standard variation (hashed) per patient group.

Figure 3: Illustration of textural parameter TC18, the Coefficient of Variation, for a set of 5 'normal' lungs (left) and a set of 5 lungs of patients suffering from COPD (right). The severity of COPD increases from top to bottom.

Figure 4: Textural parameter 18 (solid black) and standard deviation (hashed) from the invariant GLCM and for all 5 distances for the 5 patient groups studied

Figure 5: Ratio of textural parameter 30/31 (solid black) and standard deviation (hashed) from the invariant GLCM and mean over 5 distances for the 5 patient groups studied

Figure 6: High correlation between ventilated lung volume in percent and textural parameter 18 (coefficient of variation) ($r^2=0.955$).

Figure 7: Correlation between textural parameter TC13/TC31 (Variance over Mean ratio) and independent spirometry data (FeV1) for 4 of the 5 patient groups. No spirometry data was available for the 'normal' group. The quality of the linear regression is $r^2=0.66$.

FIGURE 1

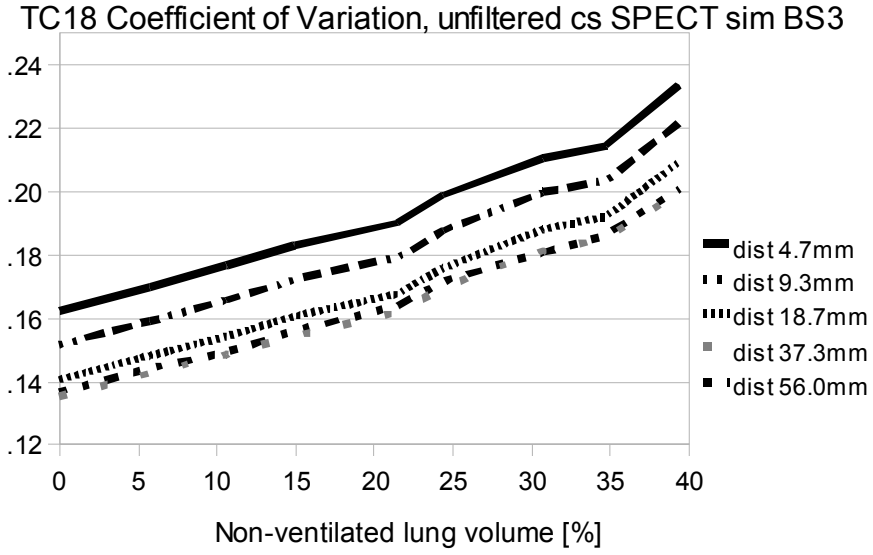


FIGURE 2

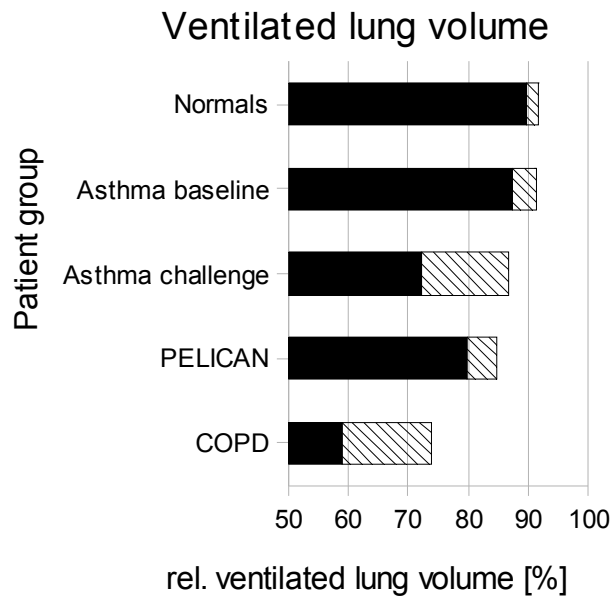


FIGURE 3 (left and right panel, reproduction in black-and-white)

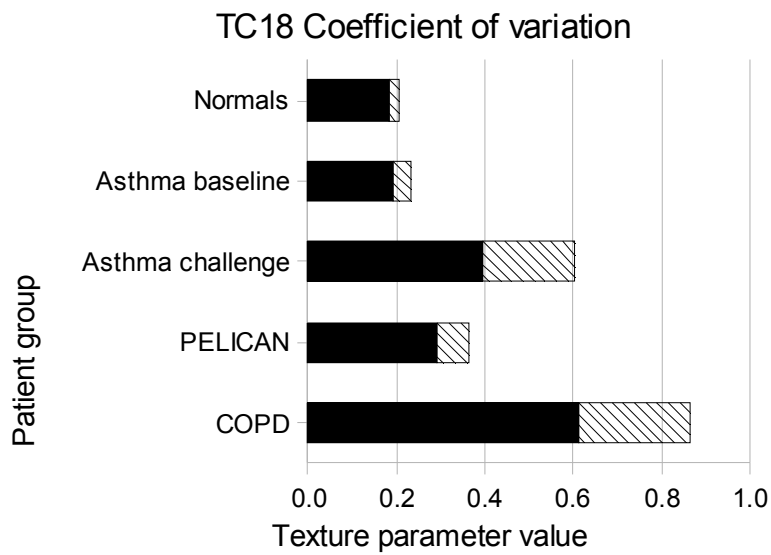
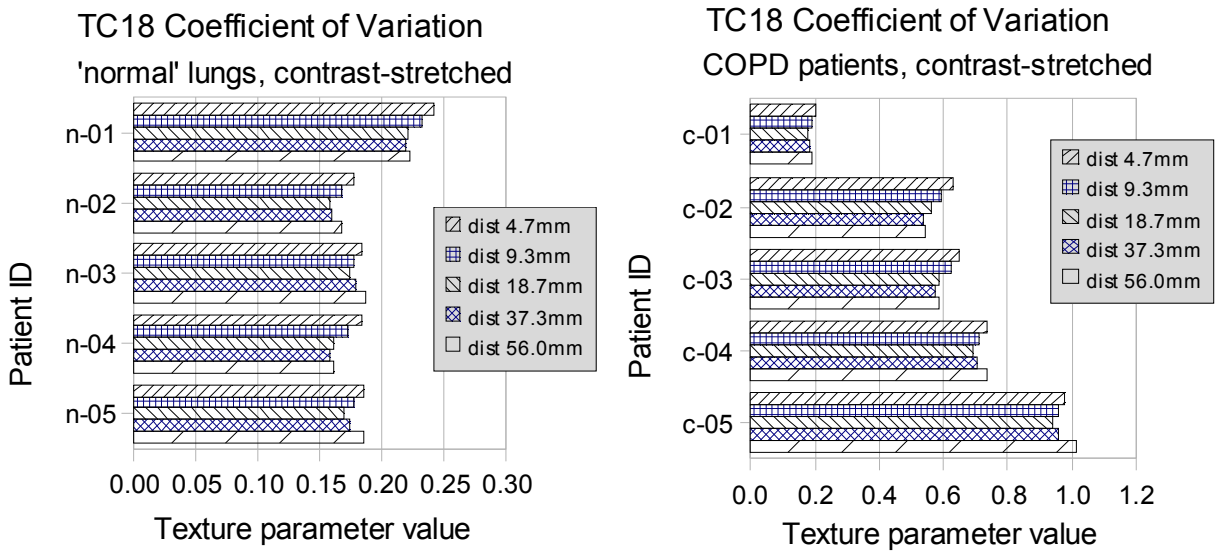


FIGURE 4

1
2
3
4
5
6
7
8
9
10
11
12
13
14
15
16
17
18
19
20
21
22
23
24
25
26
27
28
29
30
31
32
33
34
35
36
37
38
39
40
41
42
43
44
45
46
47
48
49
50
51
52
53
54
55
56
57
58
59
60
61
62
63
64
65

FIGURE 5

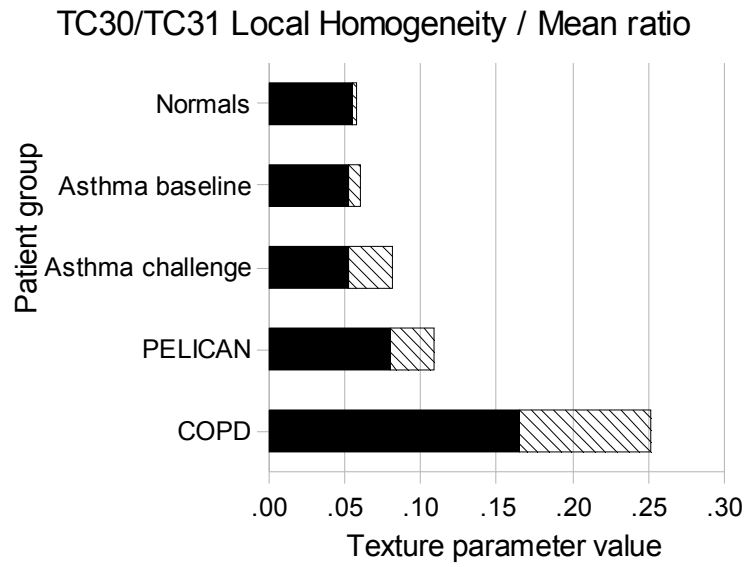


FIGURE 6 (colour reproduction for web-publishing, black-and-white for print)

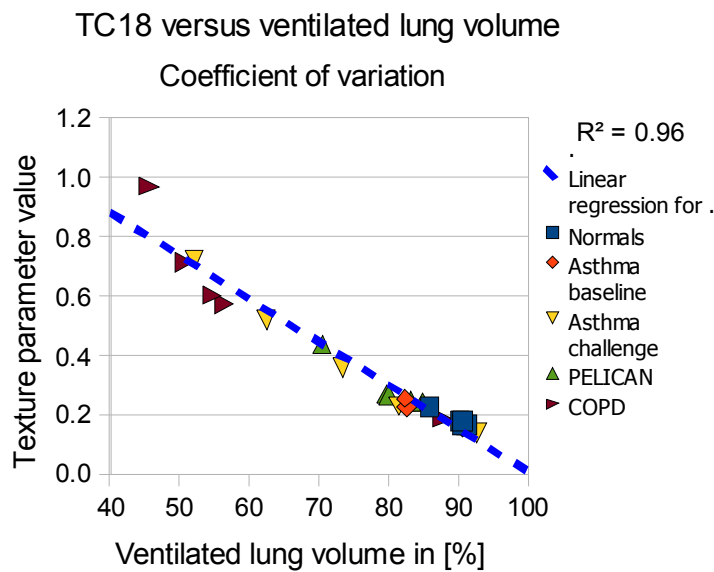
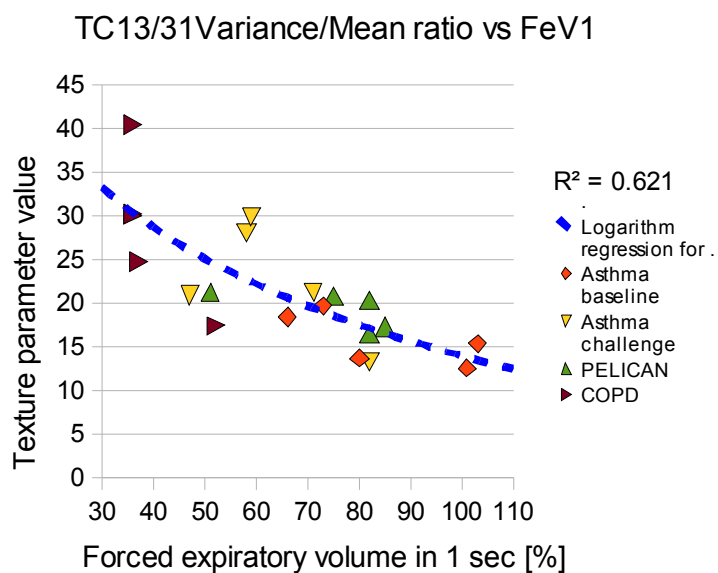


FIGURE 7 (colour reproduction for web-publishing, black-and-white for print)



Sydney, 8 December, 2008

Dr Arndt Meier
Electron Microscope Unit
Australian Key Centre for Microscopy and Microanalysis
Madsen Bldg F09, Room 270
Sydney University NSW 2006, AUSTRALIA

phone +61 2 9036 6417
fax +61 2 9351 7682
a.meier@usyd.edu.au
www.emu.usyd.edu.au

To:
The editor
Computerized Medical Imaging and Graphics

Dear editor,

we are submitting the manuscript

Application of Texture Analysis to Functional Pulmonary CT Data

Arndt Meier^a, Catherine Walsh^{b,c,d}, Benjamin E. Harris^{b,c,d}, Gregory G.King^{b,c,d}, and Allan Jones^a

- a) Australian Key Centre for Microscopy and Microanalysis, The University of Sydney, Sydney 2006, NSW, Australia, email: a.meier@usyd.edu.au (*corresponding author*)
- b) Department of Respiratory Medicine, Royal North Shore Hospital, St Leonards NSW 2065
- c) Woolcock Inst. of Medical Research, 431 Glebe Point Road, Glebe, NSW 2037
- d) Northern Clinical School, Faculty of Medicine, University of Sydney, Sydney, 2006

for publication in the journal Computerized Medical Imaging and Graphics. The work is new and genuine and has not been published previously in this or any other form nor has it been submitted to any other publisher. All studies involving human subjects have been conducted in accordance with international and local ethics requirements.

This statement is made on behalf of all authors of the manuscript.

The manuscript was prepared in OpenOffice and then exported to MS Word data format. We are additionally sending a copy in PDF format as a 'ground-truth' in the unlikely event that tables or formulas look corrupted after importing the manuscript into a genuine MS Office application. Please notify us should this happen so we can fix any problems.

We believe that the material presented is of interest to your readers and that it has been prepared in a diligent way and that it meets all criteria for submission. We are happy to clarify any questions you or the reviewers may have.

Kind Regards,

Arndt Meier